2025. Journal of Arachnology 53:30–53

A dimorphic species or underestimated diversity? *Pseudocellus pelaezi* (Coronado Gutiérrez) (Arachnida: Ricinulei: Ricinoididae) from northeastern Mexico assessed with morphological and barcoding data

Alejandro Valdez-Mondragón[1,3]*, **Griselda Montiel-Parra**[2] and **Mayra R. Cortez-Roldán**[3]: [1]Collection of Arachnology (CARCIB), Programa Académico de Planeación Ambiental y Conservación, Centro de Investigaciones Biológicas del Noroeste (CIBNOR), S.C., Km. 1 Carretera a San Juan de La Costa "EL COMITAN", La Paz, Baja California Sur. C.P. 23205, Mexico. *Email: lat_mactans@yahoo.com.mx; [2]National Collection of Acari (CNAC), Departamento de Zoología, Instituto de Biología, Universidad Nacional Autónoma de México (UNAM), Ciudad Universitaria, Apartado Postal 04510, Coyoacán, Mexico City, Mexico; [3]Laboratory of Arachnology, Laboratorio Regional de Biodiversidad y Cultivo de Tejidos Vegetales (LBCTV), Instituto de Biología, Universidad Nacional Autónoma de México (UNAM), sede Tlaxcala, Ex-Fábrica San Manuel, San Miguel Contla, 90640 Santa Cruz Tlaxcala, Tlaxcala, Mexico.

Abstract. Mexico boasts the highest number of known ricinuleid species worldwide, however the diversity from North America is still poorly known. Herein, we evaluate *Pseudocellus pelaezi* (Coronado-Gutiérrez, 1970), a dimorphic species distributed in San Luis Potosí and Tamaulipas, northeastern Mexico. This species represents the first known dimorphic species of ricinuleids, well-documented based on morphology, ultrastructure, and genetic distance. The average intraspecific genetic distance (*p*-distance) at the mitochondrial cytochrome *c* oxidase subunit 1 (CO1) within *P. pelaezi* was 4.1%, whereas a much higher value of 14.6% was found between analyzed species of *Pseudocellus* Platnick, 1980. Although the genetic distance within the species is >4%, the morphology of primary sexual structures such as the male copulatory apparatus of leg III and the female spermathecae were strongly conserved across all the specimens. However, the morphology of a secondary sexual structure, male femora II, showed variation, with some males possessing a thin femora II (morpho 1-M1) (*homeomorphic*) and others with a wide femora II (morpho 2-M2) (*heteromorphic*). This male dimorphism, even within the same population of *P. pelaezi*, might be considered as a direct effect of sexual competition among males to mate with females, however more studies are needed to test this in ricinuleids. This could be done by studying and evaluating the sexual behavior in combination with the genetic evidence from specimens across several populations, offering insight into whether such dimorphism and/or genetic variation is correlated with sexual competition or represents underestimated diversity yet to be described.

Keywords: Morphology, genetic distances, cytochrome *c* oxidase subunit 1 (CO1), morphological variation, northeastern Mexico
https://doi.org/10.1636/JoA-S-23-028

Ricinuleids are considered one of the most enigmatic and neglected arachnid orders, given their rarity and the paucity of studies on them (García et al. 2015). The ricinuleids are formally classified as Ricinulei Thorell, 1876, and are commonly referred to as "hooded tick-spiders." They represent the second least-diverse order within Arachnida, comprising 110 extant and 22 fossil species. As Botero-Trujillo et al. (2021a) mentioned, the knowledge of the diversity and abundance of these arachnids has been slow to accumulate because they are poorly represented in biological collections. While knowledge on their taxonomy and diversity has increased in the last decade (Valdez-Mondragón & Francke 2011, 2013; Valdez-Mondragón et al. 2018, 2020; Botero-Trujillo et al. 2021a, b; Valdez-Mondragón & Juárez Sánchez 2021; Valdez-Mondragón & Cortez-Roldán 2021), more fieldwork and sampling are necessary, especially in the Neotropics.

The order Ricinulei is comprised of two suborders, the extinct Palaeoricinulei Selden, 1992 and the extant and living species Neoricinulei Selden, 1992 (Selden 1992; Harvey 2003).

The superfamily Ricinoidoidea Ewing, 1929 comprises three extant genera: *Cryptocellus* Westwood, 1874 (South America), *Pseudocellus* Platnick, 1980 (Central and North America), and *Ricinoides* Ewing, 1929 (Western and Central Africa) composed of 46, 38, and 16 recognized species, respectively (Tuxen 1974; Valdez-Mondragón & Francke 2011, 2013; Valdez-Mondragón et al. 2018, 2020; Botero-Trujillo et al. 2021a, b; Valdez-Mondragón & Juárez Sánchez 2021; Valdez-Mondragón & Cortez-Roldán 2021). However, new genomic studies using ultra-conserved elements (UCEs) only recover the monophyly of *Ricinoides* whereas *Cryptocellus* and *Pseudocellus* are paraphyletic (Sato et al. in prep.).

Pseudocellus are distributed mainly in North and Central America, with some species from Caribbean islands, but most species are in Mexico (Harvey 2003; Teruel & de Armas 2008; de Armas 2017; Valdez-Mondragón & Francke 2011, 2013; Valdez-Mondragón et al. 2018, 2020; Valdez-Mondragón & Cortez-Roldán 2021; Valdez-Mondragón & Juárez-Sánchez 2021). Mexico ranks first worldwide in its number of known ricinuleid species, with 21 out of 38 described species, all belonging to the genus *Pseudocellus*. Most of the Mexican species are mainly epigean, found in the soil of lowland tropical rainforests, in the leaf litter, underlying layers of the ground, or under big rocks and under rotten logs (Harvey 2003; Valdez-Mondragón & Francke 2011, 2013; Valdez-Mondragón et al. 2018, 2020; Valdez-Mondragón & Juárez Sánchez 2021; Valdez-Mondragón & Cortez-Roldán 2021). Some species have also been found in high temperate forests, such as pine-oak, in an extensive karstic region at 2,169 m elev. (e.g., *Pseudocellus jarocho* Valdez-Mondragón & Francke, 2011).

While most of the species described from Mexico are epigean, some species inhabit caves, being true troglobites or having some kind of troglomorphisms. Mexico hosts the largest number of known troglobitic ricinuleids, with eight species: *Pseudocellus bolivari* (Gertsch, 1971), *P. boneti* (Bolívar & Pieltain, 1942), *P. monjarazi* Valdez-Mondragón & Francke, 2013, *P. osorioi* (Bolívar & Pieltain,

*(corresponding author)

Table 1.—Samples of *Pseudocellus* including *P. pelaezi* used for molecular analyses, DNA voucher numbers, localities, and GenBank accession numbers for CO1.

Species	DNA voucher	Locality	GenBank accession number
Ricinoides aff. feae		Guinea-Bissau	KR180469.1
P. boneti	130046.2	Cueva de Michapa, Town of Michapa, Morelos, Mex.	KR180451.1
P. boneti	130046	Cueva de Michapa, Town of Michapa, Morelos, Mex.	KR180446.1
P. gertschi	130036	Estación Biol. UNAM, Los Tuxlas, Veracruz, Mex.	KR180436.1
P. giribeti	80001.2	Res. Bios. El Triunfo, Camp. El Quetzal, Chis., Mex.	KR180459.1
P. giribeti	80001.1	Res. Bios. El Triunfo, Camp. El Quetzal, Chis., Mex.	KR180458.1
P. giribeti	79966.1	Res. Bios. El Triunfo, Camp. El Quetzal, Chis., Mex.	KR180457.1
P. giribeti	79891.5	4 km SE Custepec, Chis., Mex.	KR180456.1
P. giribeti	79891.4	4 km SE Custepec, Chis., Mex.	KR180455.1
P. giribeti	79891.3	4 km SE Custepec, Chis., Mex.	KR180454.1
P. giribeti	79891.2	4 km SE Custepec, Chis., Mex.	KR180453.1
P. giribeti	79891.1	4 km SE Custepec, Chis., Mex.	KR180452.1
P. giribeti	79799.4	3 km SE Custepec, Chis. Mex.	KR180450.1
P. giribeti	80243	Res. Bios. El Triunfo, Camp. El Quetzal, Chis., Mex.	KR180435.1
P. giribeti	80112	Res. Bios. El Triunfo, Camp. El Quetzal, Chis., Mex.	KR180434.1
P. giribeti	80091	Res. Bios. El Triunfo, Camp. El Quetzal, Chis., Mex.	KR180433.1
P. giribeti	79891	4 km SE Custepec, Chis., Mex.	KR180426.1
P. giribeti	79799	3 km SE Custepec, Chis., Mex.	JX951411.1
P. monjarazi	136272	Cueva de San Francisco, La Trinitaria, Chis., Mex.	KR180447.1
P. sbordonii	136270	Cueva de las Abejas, San Fernando, Chis., Mex.	KR180448.1
Pseudocellus sp.	99190	5km SE Antigua, Honduras	KR180449.1
Pseudocellus sp.	89406	5km SE Antigua, Guatemala	KR180445.1
Pseudocellus sp.	83165	Cerro Carmona, Finca El Pilar, Guatemala	KR180444.1
Pseudocellus sp.	99193	Parque Nacional La Muralla, Honduras	KR180443.1
Pseudocellus sp.	99283	Refugio El Quetzal, Guatemala	KR180442.1
Pseudocellus sp.	89422	4 km S Volcán, Atitlán, Guatemala	KR180441.1
Pseudocellus sp.	89548	5 km NW Morales, Guatemala	KR180440.1
Pseudocellus sp.	89536	5 km NW Morales, Guatemala	KR180439.1
Pseudocellus sp.	98424	13 km. E Nuevo Ocotepeque, Honduras	KR180437.1
Pseudocellus sp.	98418	Parque Nacional La Muralla, Honduras	KR180438.1
P. pelaezi	Ara0988	Outside of Cueva Ojo de Agua, Tamaulipas, Mex.	OR413818
P. pelaezi	Ara0989	Outside of Cueva Ojo de Agua, Tamaulipas, Mex.	OR413819
P. pelaezi	Ara0990	Outside of Cueva Ojo de Agua, Tamaulipas, Mex.	OR413820
P. pelaezi	Ara0991	Outside of Cueva Ojo de Agua, Tamaulipas, Mex.	OR413821
P. pelaezi	Ara0992	Outside of Cueva Ojo de Agua, Tamaulipas, Mex.	OR413822
P. pelaezi	Ara0993	Outside of Cueva Ojo de Agua, Tamaulipas, Mex.	OR413823
P. pelaezi	Ara0994	Outside of Cueva Ojo de Agua, Tamaulipas, Mex.	OR413824
P. pelaezi	Ara0995	Outside of Cueva Ojo de Agua, Tamaulipas, Mex.	OR413825
P. pelaezi	Ara0996	Outside of Cueva Ojo de Agua, Tamaulipas, Mex.	OR413826

1946), *P. oztotl* Valdez-Mondragón & Francke, 2011, *P. platnicki* Valdez-Mondragón & Francke, 2011, *P. reddelli* (Gertsch, 1971), and *P. sbordonii* (Brignoli, 1974). Other species, such as *Pseudocellus pelaezi* (Coronado Gutiérrez, 1970) or *Pseudocellus pearsei* (Chamberlin & Ivie, 1938), can be found inside caves without showing any troglomorphisms, while also being found abundant in the epigean microhabitat. Some species such as *P. pearsei* are highly abundant in caves from the Yucatan Peninsula.

Pseudocellus pelaezi is a well-studied species from northeast Mexico described by Pittard & Mitchell (1972) from the caves Cueva del Taninul I in San Luis Potosi and Cueva de la Florida in Tamaulipas. They gave a detailed comparative morphological description of the different life stages, providing important morphological data such as well-illustrated somatic and cuticular descriptions, as well as internal anatomy data. Furthermore, they describe *P. pelaezi* as a dimorphic species, with two male morphotypes. However, the authors do not provide additional explanation regarding the cause of such dimorphism.

For centuries, evolutionary studies have sought to understand sexual dimorphism and how sexual features among sexes are naturally selected (Darwin 1871; Wallace 1889). In the last 40 years, research has focused on understanding the widespread variation among individuals within the two sexes, leading sexual variation to be understood as the differences exhibited between males and females or within each individual sex (Andersson 1994; Barraclough et al. 1995; Gross 1996; Huber 2021). However, sexual variation within sexes, along with any potentially differing sexual behaviors exhibited, has not been studied for certain groups including ricinuleids. As such, the implications of this morphological variation in the behavior of individuals is unknown in most cases.

The objective and relevance of this work is to provide morphological and additional molecular evidence—for the very first time in Ricinulei—to support the claim of the male dimorphism in *Pseudocellus pelaezi*, a North American species from Mexico, under an integrative approach.

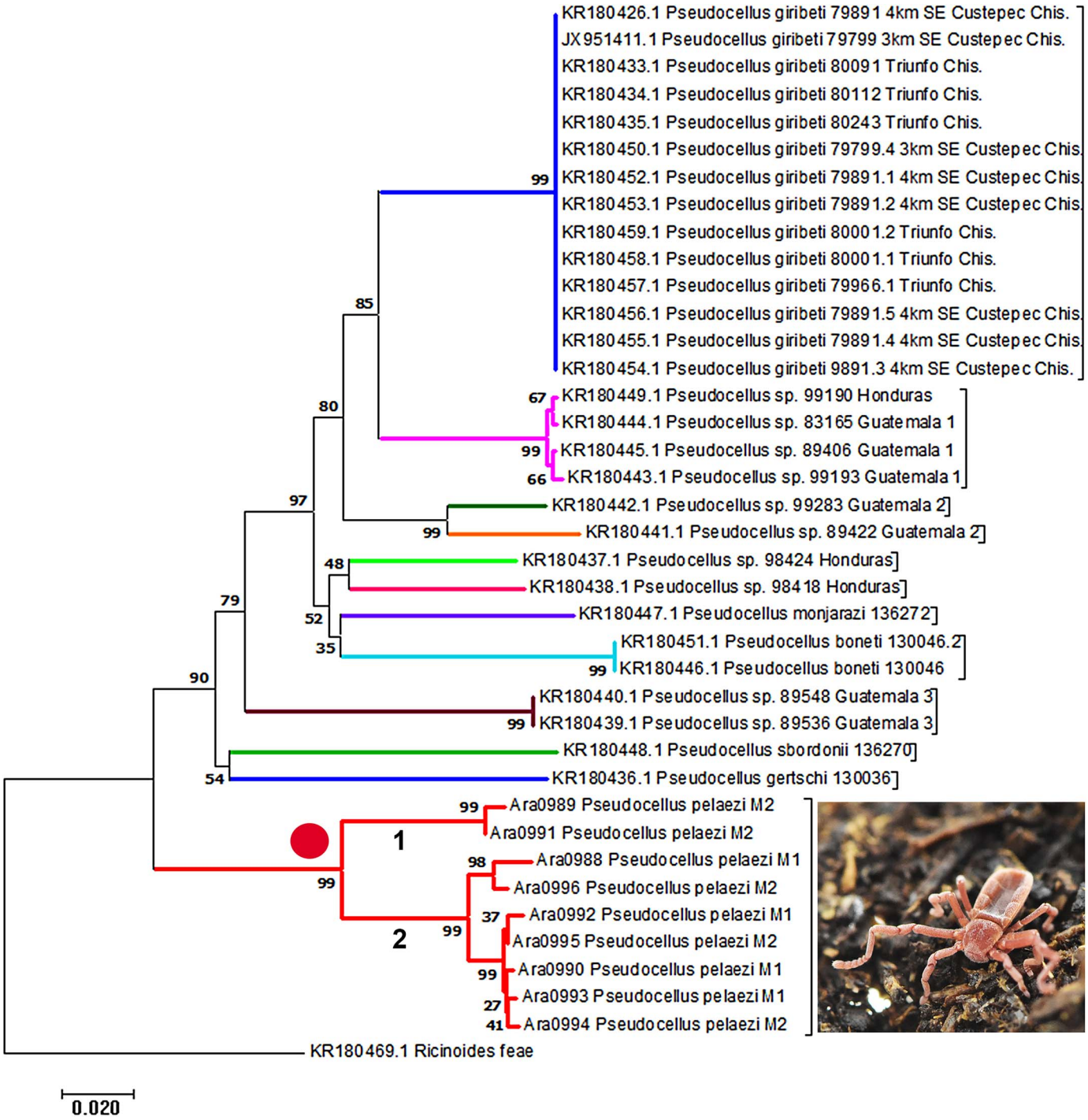

Figure 1.—Neighbour-Joining (NJ) tree with *p*-distances constructed with CO1 barcode sequences from different specimens and species of *Pseudocellus*. Branch colors indicate different species of *Pseudocellus*, with the red branches indicating specimens of *P. pelaezi*, morpho 1 (M1) and morpho 2 (M2). Small numbers on the branches represent Bootstrap support values (>50% significant). Big numbers on the branches represent the two groups of *P. pelaezi* discussed in the text.

METHODS

Biological material.—The collected specimens were deposited in 80% ethanol after being labeled with complete field data and collection codes in the Colección Nacional de Arácnidos (CNAN), Institute of Biology, Universidad Nacional Autónoma de México (IBUNAM), Mexico City, Mexico and the Colección de Aracnología y Entomología (CARCIB), Centro de Investigaciones Biológicas del Noroeste, CIBNOR S.C., La Paz, Baja California Sur, Mexico. Additional institutions mentioned herein include Escuela Nacional de Ciencias Biológicas (ENCB) and Instituto Politécnico Nacional (IPN).

Table 2.—Genetic *p*-distance under NJ of CO1 within *Pseudocellus pelaezi* samples. Average *p*-distance = 4.1%. Morpho 1 (M1). Morpho 2 (M2). Bold letters indicate samples that belong to group 1 in the tree (see Fig. 1 and text for details).

Species	1	2	3	4	5	6	7	8
1. Ara0988 *P. pelaezi*–M1								
2. Ara0989 *P. pelaezi*–M2	0.096							
3. Ara0990 *P. pelaezi*–M1	0.025	0.083						
4. Ara0991 *P. pelaezi*–M2	0.086	0.000	0.080					
5. Ara0992 *P. pelaezi*–M1	0.025	0.089	0.007	0.079				
6. Ara0993 *P. pelaezi*–M1	0.025	0.085	0.005	0.079	0.010			
7. Ara0994 *P. pelaezi*–M2	0.023	0.091	0.005	0.078	0.008	0.005		
8. Ara0995 *P. pelaezi*–M2	0.020	0.080	0.002	0.085	0.000	0.000	0.000	
9. Ara0996 *P. pelaezi*–M2	0.010	0.094	0.023	0.083	0.026	0.023	0.024	0.018

Observations and identifications of specimens were performed using a Zeiss Discovery V8 stereomicroscope. A Zeiss Axiocam 506 color camera attached to a Zeiss AXIO Zoom V16 stereomicroscope was used to photograph morphological structures. All measurements are in millimeters (mm). Photography was conducted with specimens and structures submerged in commercial-use gel alcohol (to hold them in the appropriate position), while specimens were completely covered with liquid 80% ethanol for preparation. Spermathecae were dissected and cleaned using KOH-10%.

For photomicrographs, morphological structures were dissected and cleaned with an ultrasonic cleaner at 20–40 kHz; subsequently, they were critical-point dried and examined at low vacuum with a Hitachi S-2460N scanning electron microscope (SEM). All scale measurements on photomicrographs are in micrometres (μm). Digital images were edited in Adobe Photoshop CS6. The distribution map was produced using SimpleMappr (Shorthouse 2010).

Terminology used for referring to leg segments follows Gertsch (1971), whereas for copulatory and somatic structures, we follow Pittard & Mitchell (1972), Valdez-Mondragón & Juárez-Sánchez (2021), and Valdez-Mondragón & Cortez-Roldán (2021): ac, accessory piece of the male copulatory apparatus of leg III; Lc, lamina cyathiformis; mP, metatarsal process; MT, metatarsus; and tP, tarsal process. We use the following abbreviations for cuticular structures on the male copulatory apparatus and body following Talarico et al. (2006) and Salvatierra & Tourinho (2016): BS, barbed setae; CT, conical tubercles; CS, curved and wide setae; FD, flat depressions; FT, flattened tubercles. LC, long curved-tip setae; LP, long and porous setae; LS, lamellar setae; LSO, mechanoreceptor long slit organs; Mic, microtrichia; OS, ordinary setae; SD, dome-like tubercles; TS, tree-like setae.

Taxon sampling: The molecular analyses are based on a total of 39 samples from 12 species, including *P. pelaezi* and one single outgroup just to root the tree: *Ricinoides* aff. *feae* (Hansen, 1921). The samples used in the molecular analyses are listed in Table 1. All CO1 (cytochrome c oxidase subunit 1 (CO1)) sequences were downloaded from GenBank, except the sequences of *P. pelaezi* (OR413818–OR413826) which were generated for this study (Table 1).

DNA extraction, amplification, and sequencing: For DNA extraction, we used the Qiagen DNeasy extraction kit, following the modifications suggested by Nolasco & Valdez-Mondragón (2022). One leg from each specimen was used for DNA extraction, using only adult specimens. Amplification of the CO1 barcoding marker was carried out using the primers: LCO1490/HCO2198 (Folmer et al. 1994). Polymerase chain reactions (PCR) were performed in a Verity-Applied Biosystems 96 Well Thermal Cycler, using the Qiagen Multiplex PCR kit (Hilden, Germany). The final volume of each PCR reaction was 20 μl: 2.3 μl H_2O, 2.0 μL 5X Q-solution, 10 μL 2X Multiplex PCR Master Mix (providing a final concentration of 3 mM $MgCl_2$), 1.6 μl each of the forward and reverse primers (10 nM stock solution), and 2.5 μl of extracted DNA sample. The cycles and optimal temperatures for CO1 amplification were as follows: Initial heating phase of 15 min at 95°C, 35 amplification cycles of 35 s at 94°C (denaturing), 1 min 30 s at 40°C (annealing), and 1 min 30 s at 72°C (elongation), with a final elongation of 10 min at 72°C. Gel electrophoresis was carried out on 0.5% agarose gels (Millipore Agarose for analytical nucleic acid electrophoresis) in TBE buffer, using the molecular weight marker Perfect DNA 100 bp

Table 3.—Linear measurements (mm) and averages of the analyzed specimens for morpho 1 males (M1), morpho 2 males (M2), and females. Ind = Individual, Tl = total length, Cl = carapace length, Cw = carapace width, Cul = cucullus length, Cuw = cucullus width, Opl = opisthosoma length, Opw = opisthosoma width, FII (l/d) = femur II (length/width). Bold numbers represent maximum and minimum values.

Ind	Tl	Cl	Cw	Cul	Cuw	Opl	Opw	FII (l/d)
				Males				
M1								
1	3.8	1.15	1.12	0.55	0.85	2.55	1.50	3.11
2	3.6	**1.25**	1.15	0.52	0.85	2.45	1.45	3.0
3	3.65	1.20	**1.20**	**0.55**	**0.85**	**2.60**	**1.55**	**2.80**
4	**3.25**	**1.10**	**1.10**	**0.50**	**0.80**	**2.25**	**1.40**	**4.3**
Average=	3.57	1.17	1.14	0.53	0.83	2.46	1.47	3.30
M2								
1	3.60	1.22	1.20	0.55	0.85	2.50	**1.60**	2.80
2	3.65	1.22	1.20	0.55	0.80	2.55	1.55	**3.00**
3	**3.70**	**1.25**	**1.20**	0.55	**0.85**	2.55	1.52	**2.63**
4	3.67	1.20	1.20	0.55	0.85	2.52	1.55	2.90
5	3.65	1.22	1.20	**0.57**	0.85	**2.60**	1.55	2.70
6	**3.55**	**1.15**	**1.15**	**0.52**	**0.80**	**2.47**	**1.50**	2.84
Average=	3.64	1.21	1.19	0.55	0.83	2.53	1.55	2.81
				Females				
1	**3.47**	**1.10**	1.20	**0.50**	**0.82**	**2.40**	**1.60**	5.12
2	3.67	1.25	**1.25**	0.55	0.87	2.47	1.67	5.20
3	3.65	1.17	1.20	0.52	0.85	2.55	1.72	**5.40**
4	3.55	1.20	1.20	0.55	0.85	2.47	1.65	5.00
5	3.55	1.20	1.20	0.55	0.85	2.45	1.65	5.00
6	3.67	1.25	1.20	0.55	0.90	**2.60**	1.70	5.00
7	**3.72**	**1.27**	1.25	**0.57**	**0.90**	2.55	1.75	5.09
8	3.67	1.17	**1.17**	0.55	0.80	2.55	1.65	5.40
9	3.60	1.20	1.22	0.55	0.90	2.50	1.67	**4.72**
10	3.72	1.25	1.25	0.50	0.87	2.57	**1.77**	5.09
Average=	3.627	1.206	1.214	0.539	0.861	2.511	1.683	5.102

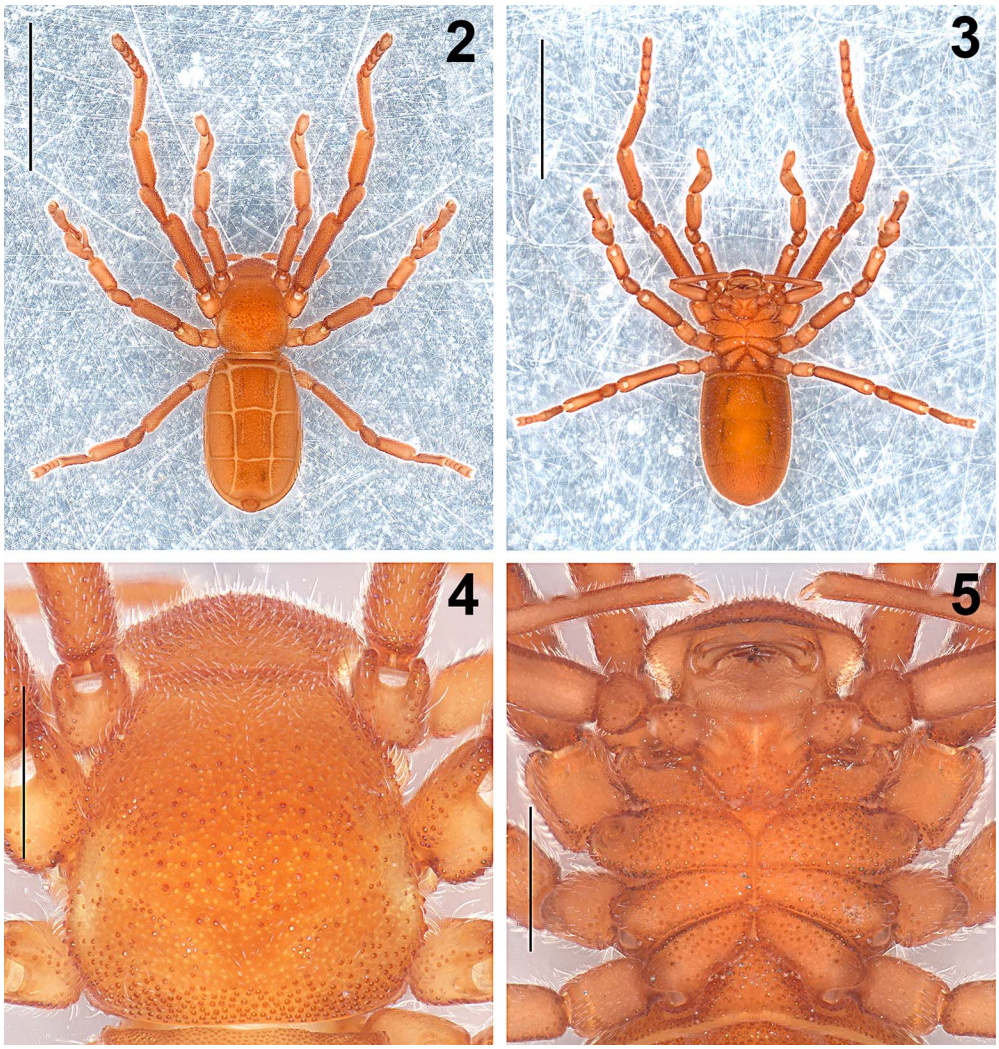

Figures 2–5.—*Pseudocellus pelaezi,* male, morpho 1 (M1). 2–3. Habitus, dorsal and ventral views. 4. Carapace, dorsal view. 5. Prosoma, ventral view, showing coxosternal region. Scale bars: 2–3 = 2 mm; 4–5 = 0.5 mm.

Ladder (Novagen) to calculate fragment size of amplifications. Gels were visualized in a photodoc BioDoc-It2 Imager 315 Imaging System LMS-20 Transilluminator. PCR products were purified using a QIAquick Qiagen purification kit. Tissue selection, DNA extraction, amplification, and purification were performed at the Laboratory of Molecular Biology at Laboratorio Regional de Biodiversidad y Cultivo de Tejidos Vegetales (LBCTV), IB-UNAM, Tlaxcala City. Sanger sequencing was carried out at the Laboratory of Molecular Biology and Health, IB-UNAM, Mexico City.

DNA sequence alignment and editing: Both DNA strands (forward and reverse) were sequenced. DNA sequences were edited in BioEdit v.7.0.5.3 (Hall 1999) and Geneious v.8.1.9 (Rozen & Skaletsky 1999). A multiple alignment of sequences was implemented using the MAFFT v.7 (Katoh & Toh 2008) online version (https://mafft.cbrc.jp/alignment/server/) with the following commands: Auto (FFT-NS-2, FFTNS-I, or L-INS-I, depending on data size). In some cases, the alignment was edited in BioEdit v.7.0.5.3. The aligned matrix in FASTA format was subsequently used in the molecular analyses.

Molecular analysis.—A phenetic molecular analysis using DNA Barcoding (CO1) was implemented under the corrected *p*-distances neighbor-joining (NJ) criteria. A genetic distance tree was reconstructed using MEGA v. 10.1.7 (Kumar et al. 2018) under the following parameters: Number of replicates = 1000, Bootstrap support values = 1000 (significant values ≥ 50%), Substitution type = nucleotide, Model = p-distance, Substitution to include = d: Transitions + Transversions, Rates among sites = Gamma distributed with invariant sites (G+I), Missing data treatment = Pairwise deletion, Select Codon Position: 3rd.

Morphological analysis.—Eight body linear measurements (mm) were considered to study the morphological variation within dimorphic males and between males and females: (1) total length (carapace + opisthosoma including pygidium), (2) carapace length, (3) carapace width (widest part), (4) cucullus length, (5) cucullus width, (6) opisthosoma length, (7) opisthosoma width (widest part) (not including pygidium), and (8) femur II length/diameter (l/d). The measurements were taken under a stereoscope Stemi SR ZEISS.

RESULTS

Molecular analyses.—The analyzed CO1 matrix was composed of 39 terminals (including one outgroup) and 655 aligned

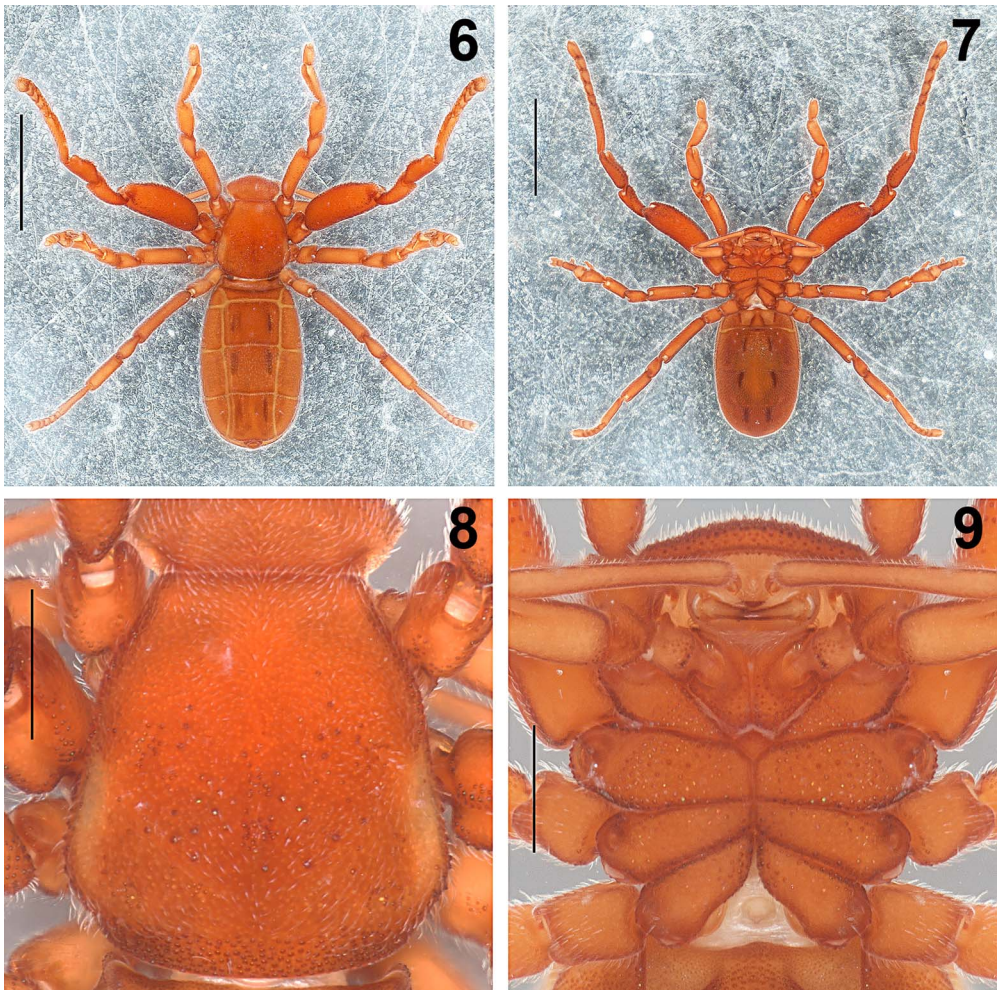

Figures 6–9.—*Pseudocellus pelaezi,* male, morpho 2 (M2). 6–7. Habitus, dorsal and ventral views. 8. Carapace, dorsal view. 9. Prosoma, ventral view, showing coxosternal region. Scale bars: 6–7 = 2 mm; 8–9 = 0.5 mm.

characters. The matrix used in the molecular analyses was the same as that implemented by Valdez-Mondragón & Cortez-Roldán (2021) for the delimitation and description of *Pseudocellus giribeti* Valdez-Mondragón & Cortez-Roldán 2021, with the addition of nine new sequences of *P. pelaezi* (Table 1). The average genetic distance among analyzed species of *Pseudocellus* was 14.6% under NJ. Bootstrap support values were high for the monophyly of *P. pelaezi* samples (99%) (Fig. 1). The average intraspecific genetic variation within *P. pelaezi* was found to have a p-distance of 4.1% (Table 2). The average p-distance between groups 1 and 2 within *P. pelaezi* was 8.5% (Fig. 1), whereas the within-group distance for group 1 and 2 was 0.0% and 1.3%, respectively (Fig. 1). Each group (1 and 2) within *P. pelaezi* was supported with high Bootstrap values (99%) (Fig. 1).

Morphology.—A total of 35 specimens of *P. pelaezi* were examined to assess the morphological variation among dimorphic males, as well as between males and females. Not all measurements were taken from every specimen because some were broken or incomplete. The specimens used for linear measurements are presented in Table 3. All specimens were collected from the same locality (Cueva de Ojo de Agua, Tamaulipas, Mexico) but on different dates, therefore all specimens belong to the same dimorphic population. Specimens were classified as morpho 1 (M1) or morpho 2 (M2). M1 represents the smaller specimens and M2 the larger ones (Table 3).

Males.—Body coloration was similar between both morphs M1 and M2, being reddish in live specimens and orange under the stereomicroscope (Figs. 2–9). Total length was slightly smaller in M1 males than M2 males, with an average of 3.57 mm and 3.64 mm, respectively (Table 3).

Carapace: M1 males with carapace more oval than M2 males (Figs. 4, 60, 61), which are trapezoidal (Fig. 8). Also, translucent areas present at level of trochanters II are slightly more visible in M2 than M1 (Figs. 4, 8). Carapace in M2 is slightly longer and wider than M1 in most specimens (Table 3). No differences were found in the cuticular structures under SEM between M1 and M2, both having the flattened tubercles (FT) on the median groove and the ordinary setae (OS) (Figs. 60, 61, 63–65).

Sternal region: No differences were found between M1 and M2, both with coxae covered with translucent setae and granules similar to those on carapace (Figs. 3, 5, 7, 9). Coxae I rhomboidal, II sub-rectangular, III and IV conical. Coxae II larger and wider than others. Coxae II meets tritosternum along one-third of its length (Figs. 5, 9).

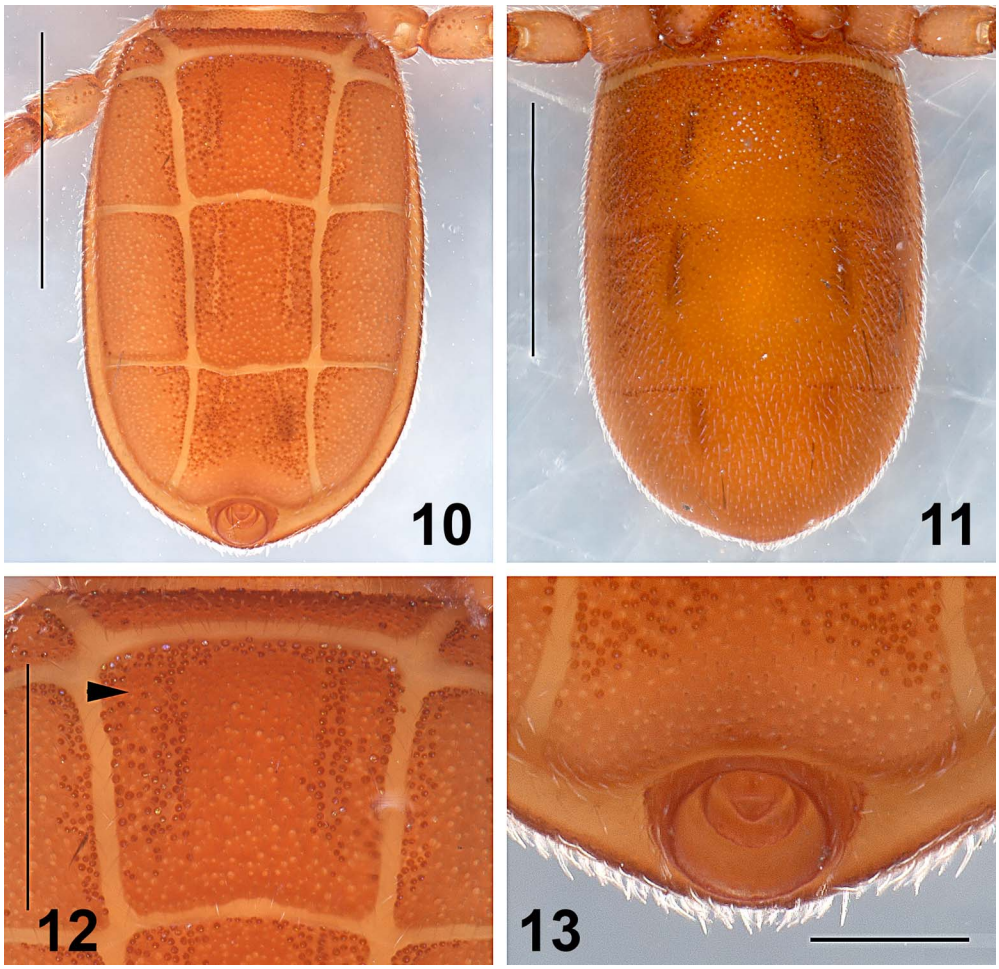

Figures 10–13.—*Pseudocellus pelaezi*, male, morpho 1 (M1). 10–11. Opisthosoma, dorsal, and ventral views. 12. Tergite XI, median plate (arrow indicates the lateral depression). 13. Pygidium, posterior view. Scale bars: 10–11 = 1 mm; 12 = 0.5 mm; 13 = 0.2 mm.

Opisthosoma: The opisthosoma in M2 is slightly longer and wider than in M1 in most specimens (Figs. 10–12, 14–16) (Table 3), however, the tergite XII in M1 tends to be slightly longer than in M2 (Figs. 10, 14). No differences were found in the cuticular structures under SEM between M1 and M2, both with small pits and translucent setae (Figs. 60, 62, 87, 88).

Cucullus and chelicerae: The cucullus in M1 is as longer as wider than in M2 in most specimens (Table 3), however the shape is a little bit different, with M1 having more rounded edges than in M2 (Figs. 27, 28). No differences were found in the cuticular structures under SEM between M1 and M2, with both having the pits, ordinary setae (OS) and the dome-like tubercles (SD) on apical region (Figs. 66–68). As for the chelicerae, no differences were found in the size of the fixed and movable finger, with both having the same number and size of teeth (Figs. 19, 28). Under SEM, no differences were found in the cuticular structures, with both having tree-like setae (TS) close to the chelicerae (Figs. 69–71).

Palps and legs: In both morphos (M1 and M2), the palps do not show any variation in the shape (Figs. 25, 26, 34, 35). Under SEM, no differences were found in the cuticular structures, with both morphos presenting the mechanoreceptor long slit organs (LSO) (Figs. 83–86). In the tibia II and metatarsus II, no differences were found, although some specimens of M2 (Figs. 29–32) have ventral scattered sharp-tipped granules slightly longer than in M1 (Figs. 20–23). The femora II are wider in M2 than in M1 as previously reported by Pittard & Mitchell (1972) (Figs. 24, 33). The femora II in M2 are on average 2.81 times longer than wide, whereas in M1 this structure is on average 3.30 times longer than wide (Table 3). Under SEM, no differences were found in the cuticular structures, with both showing pits and ordinary setae (OS) (Figs. 72, 73).

Leg III and copulatory apparatus: In regard to the copulatory apparatus, the tarsal process (tP) is basically the same in both M1 (Figs. 37–41) and M2 (Figs. 43–47) morphos in prolateral and dorsal views, both with a sinuous shape in prolateral view with the same two lobules on the distal part (arrows Figs. 39, 40, 45, 46) and under SEM (Figs. 74, 76, 77). Apically, the accessory piece (ac) of the tP shows the same harpoon shaped in M1 (Figs. 39, 40) and M2 (Figs. 45, 46). However, differences in the shape of the metatarsal process (mP) were observed, being longer in M2 (Fig. 43) than in M1 (Fig. 37). Also, the lamina cyathiformis (Lc) in M2 (Fig. 42) is longer, thinner, and more triangular than in M1 (Fig. 36). Under SEM, no differences were found in the cuticular structures of the

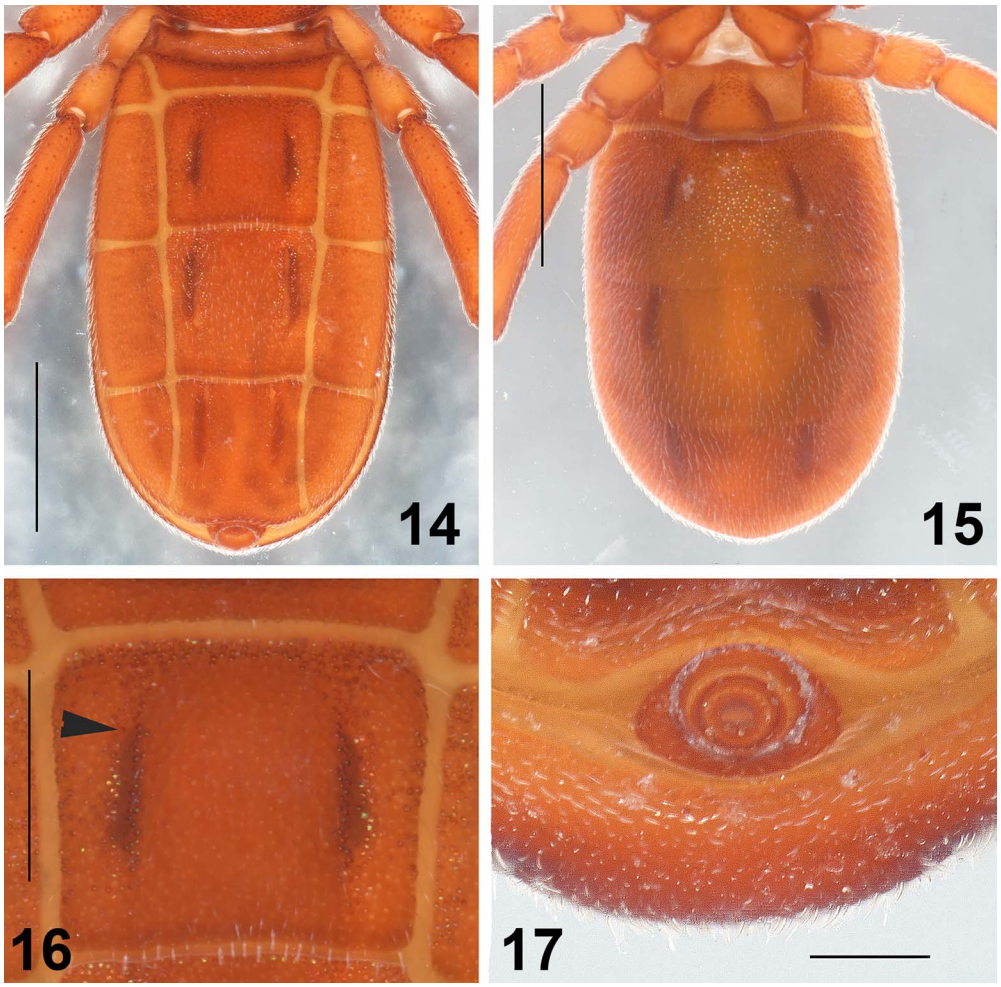

Figures 14–17.—*Pseudocellus pelaezi*, male, morpho 2 (M2). 14–15. Opisthosoma, dorsal, and ventral views. 16. Tergite XI, median plate (arrow indicates the lateral depression). 17. Pygidium, posterior view. Scale bars: 14–15 = 1 mm; 16 = 0.5 mm; 17 = 0.2 mm.

legs, showing the lamellar setae (LS) along the tarsus of leg III (Fig. 78), the long curved-tip setae (LC), and the long and porous setae (LP) (Figs. 78, 79). In both morphos, conical tubercles (CT) and flat depressions (FD) were observed on the distal part of tarsus III of leg III (Figs. 78, 80, 82), while curved and wide setae (CS) were present on the ventral part of tarsus IV of leg III (Figs. 79, 81). No variation in the microtrichia (Mic) was observed on tarsus III of leg III (Figs. 80, 82).

Females.—*General morphology:* Overall, the females showed the same general morphology, with no evidence of dimorphic females; however, some specimens presented darker coloration than others (Figs. 48, 49, 54, 55). Also, the body coloration in males is slightly darker than in females. The carapace shape was the same among the analyzed females (Figs. 48, 54, 89). Under SEM, no differences were found in the cuticular structures of the legs, which were similar to the males in having lamellar setae (LS), long and porous setae (LP), conical tubercles (CT), flat depressions (FD), mechanoreceptor long slit organs (LCO), long curved-tip setae (LC) and barbed setae (BS) on ventral part of tarsus (Figs. 90–92).

Within the females, little morphological variation was observed in most of body measurements (Table 3), suggesting no dimorphism in females. Females had almost the same length as M2 males (x = 3.62 in females vs. x = 3.64 in M2) but were longer than M1 (x = 3.62 in females vs. x 3.57 in M1) (Table 3). The femora II (l/d) were considerably thinner in females (4.72–5.40, x = 5.10) than in M1 males (2.80–4.30, x = 3.30) and M2 males (2.63–3.00, x = 2.81) (Table 3).

Spermathecae: The spermathecae were basically the same across all analyzed females with no differences found (Figs. 50–53, 56–59). The spermathecae has four lobules on each side, with the external lobules being rounded and bigger than the internal ones, which are oval-shaped (Figs. 50–53, 56–59).

Taxonomic summary

Genus *Pseudocellus* Platnick, 1980

Type species.—*Pseudocellus dorotheae* (Gertsch & Mulaik, 1939).

Pseudocellus pelaezi (Coronado-Gutiérrez 1970)

Cryptocellus pelaezi Coronado Gutierrez 1970: 48–61, figs 1–9; Mitchell 1970: 63–74; Reddell 1971: 34; Reddell & Mitchell

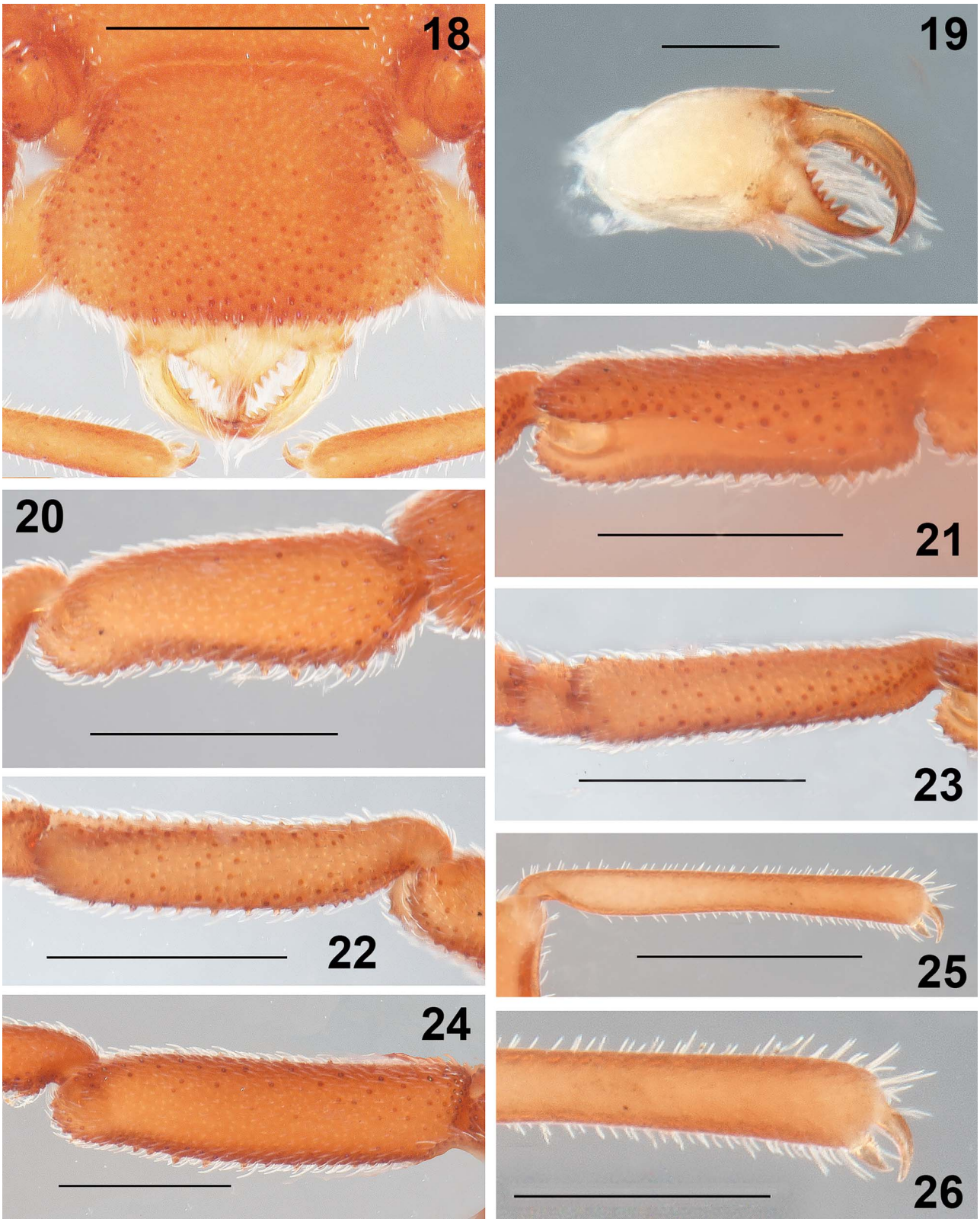

Figures 18–26.—*Pseudocellus pelaezi*, male, morpho 1 (M1). 18. Cucullus, dorsal view. 19. Left chelicera, dorsal view. 20–21. Right tibia II, prolateral and proventral views. 22–23. Right metatarsus II, prolateral and proventral views. 24. Right femur II, prolateral view. 25. Right pedipalp tibia, retrolateral view. 26. Detail of the movable and fixed claws of the right pedipalp, retrolateral view. Scale bars: 18, 20–25 = 0.5 mm; 19 = 0.2 mm; 26 = 0.1 mm.

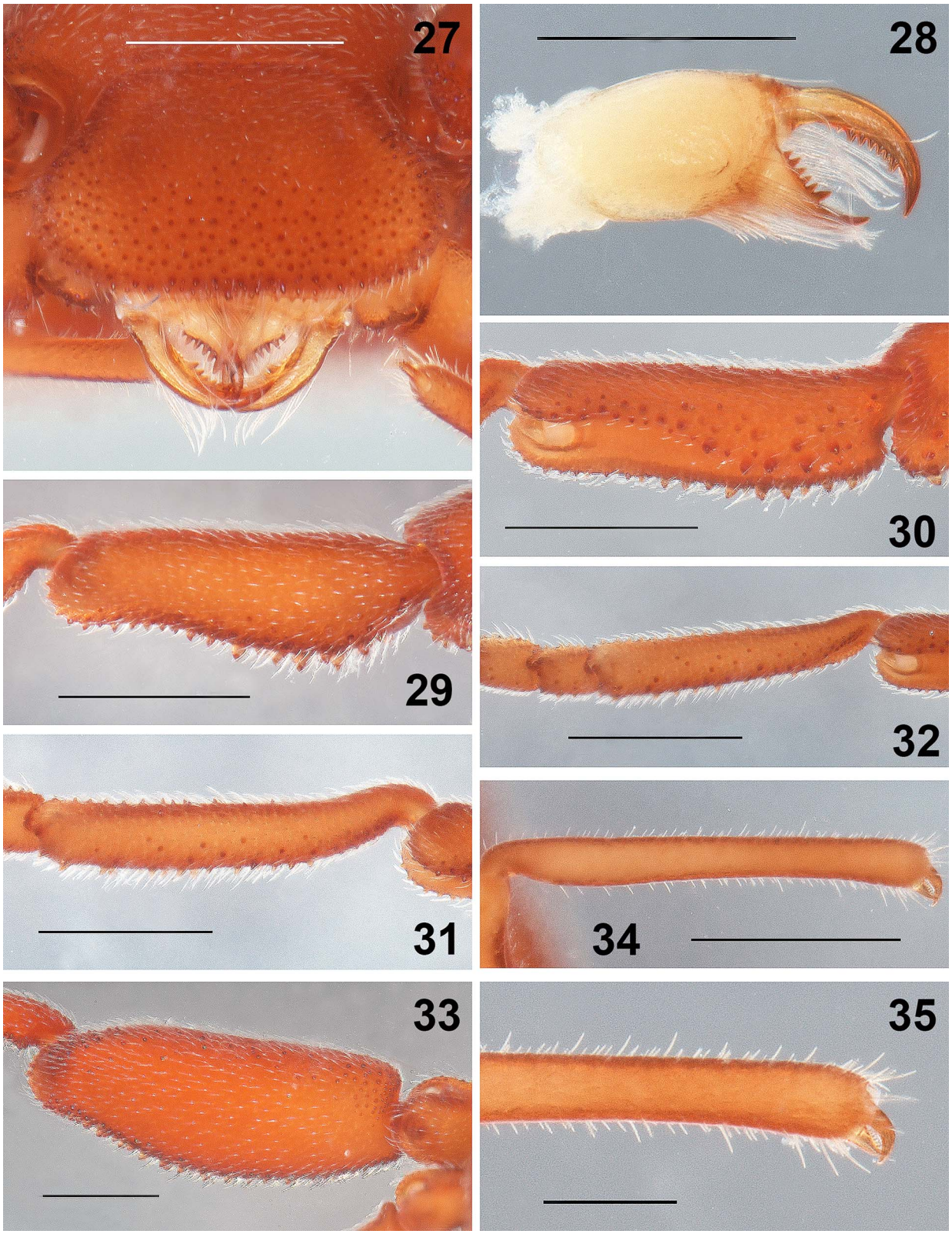

Figures 27–35.—*Pseudocellus pelaezi*, male morpho 2 (M2). 27. Cucullus, dorsal view. 28. Left chelicera, dorsal view. 29–30. Right tibia II, prolateral and proventral views. 31–32. Right metatarsus II, prolateral and proventral views. 33. Right femur II, prolateral view. 34. Right pedipalp tibia, retrolateral view. 35. Detail of the movable and fixed claws of the right pedipalp, retrolateral view. Scale bars: 27, 29–34 = 0.5 mm; 28 = 0.2 mm; 35 = 0.1 mm.

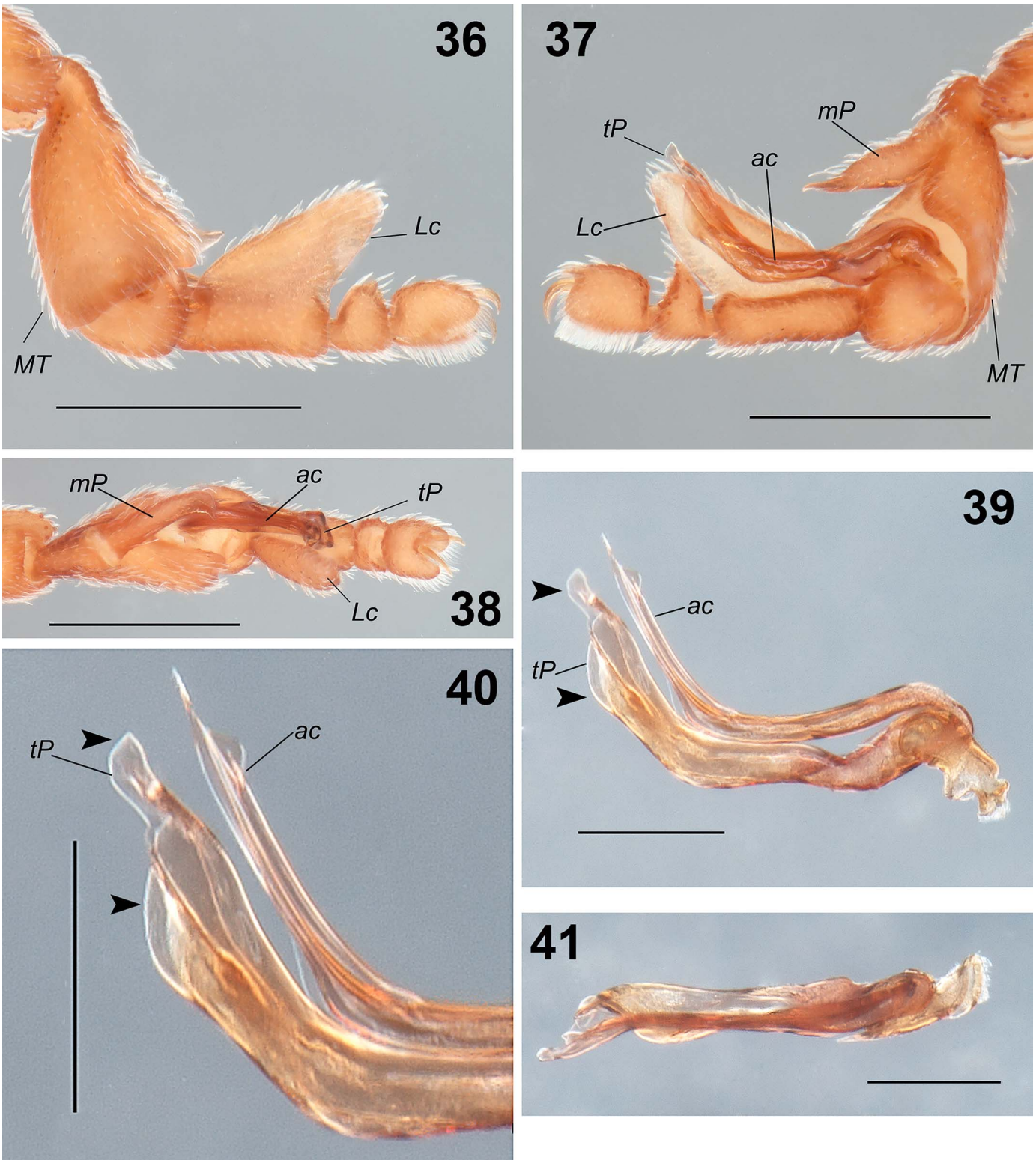

Figures 36–41.—*Pseudocellus pelaezi* morpho 1 (M1). 36–38. Right leg III (copulatory apparatus), retrolateral, prolateral and dorsal views respectively. 39. Copulatory apparatus extended, prolateral view. 40. Copulatory apparatus, apical detail. 41. Copulatory apparatus, dorsal view. Arrows indicate the two distal lobules on the tP. Scale bars: 36–38 = 0.5 mm; 39, 41 = 0.2 mm; 40 = 0.1 mm.

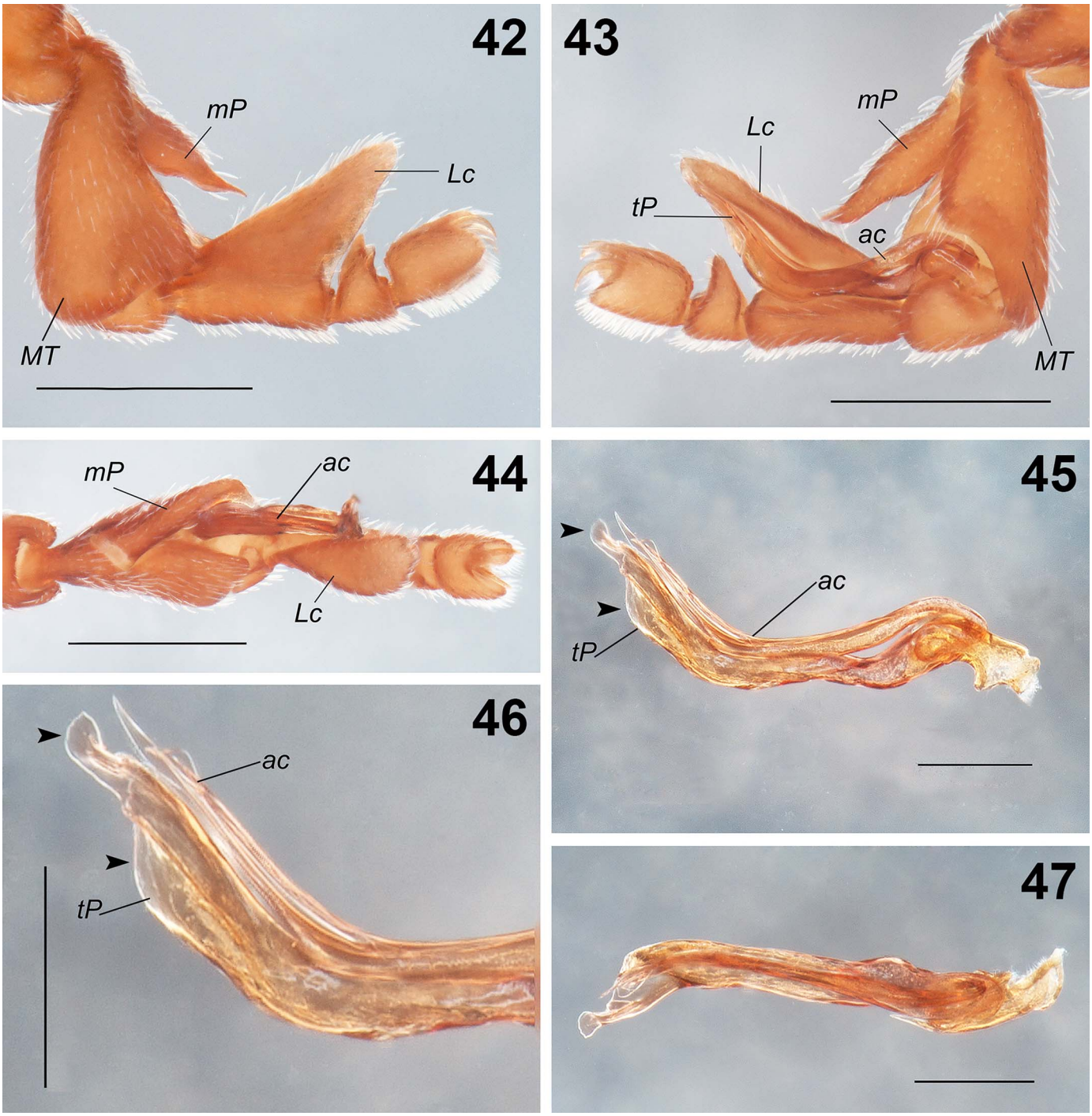

Figures 42–47.—*Pseudocellus pelaezi* morpho 2 (M2). 42–44. Right leg III (copulatory apparatus), retrolateral, prolateral and dorsal views respectively. 45. Copulatory apparatus, prolateral view. 46. Copulatory apparatus, apical detail. 47. Copulatory apparatus, dorsal view. Arrows indicate the two distal lobules on the tP. Scale bars: 42–44 = 0.5 mm; 45, 47 = 0.2 mm; 46 = 0.1 mm.

1971: 148, fig. 7; Pittard & Mitchell 1972: 1–77, figs 1–130; Reddell & Elliott 1973: 175; Brignoli 1974: 157, fig. 1a; Reddell 1981: fig. 45; Woolley 1988: fig. 3–4h; Canard & Stockmann, 1993: fig. 7 (as *Cryptocellus palaezi* [sic]); Juberthie 1994: 232, 233, 234, figs 2 (labelled 'fig. 1'), 3.

Pseudocellus pelaezi (Coronado): Platnick 1980: 352; Humphreys 1995: 178, figs 2d–f (as *Pseudocellus palaezi* [sic]); Vázquez-Rojas 1995: 27, 28; Dunlop 1996: figs 1, 3, 5, 7, 9; Vázquez Rojas 1996: 80, 81.

Figs. 2–92

Type material.—*MEXICO: San Luis Potosi* 1 ♂, 1 larva (ENCB-IPN) [16.xii.1950; F. Bonet Col.] from Cueva del Taninul (21.9369°, −98.8903°), tropical rainforest. Not examined.

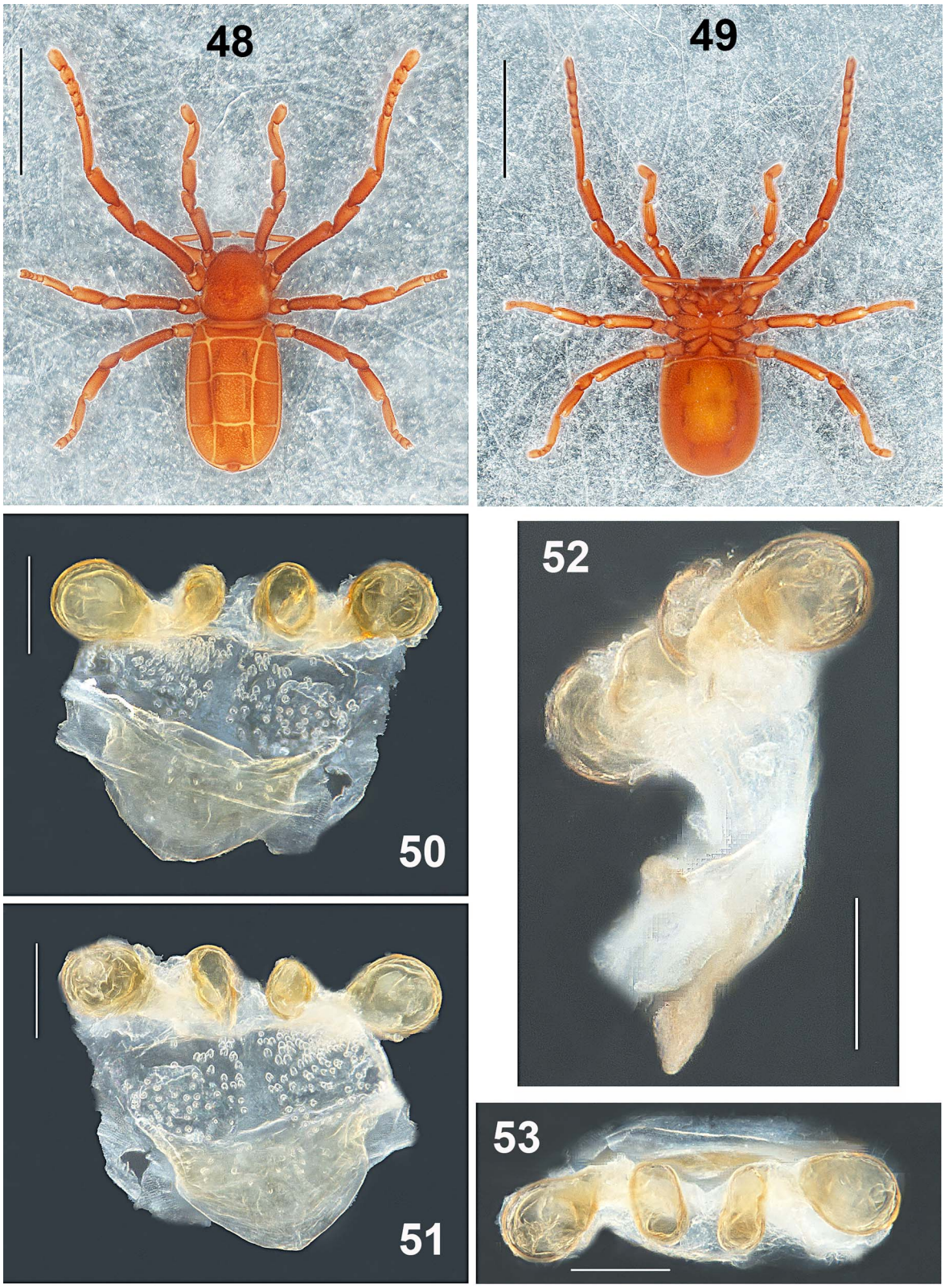

Figures 48–53.—*Pseudocellus pelaezi*, female 1. 48–49. Habitus, dorsal and ventral views. 50–53. Spermathecae, anterior, posterior, lateral and dorsal views, respectively. Scale bars: 48–49 = 2 mm; 50–53 = 0.2 mm.

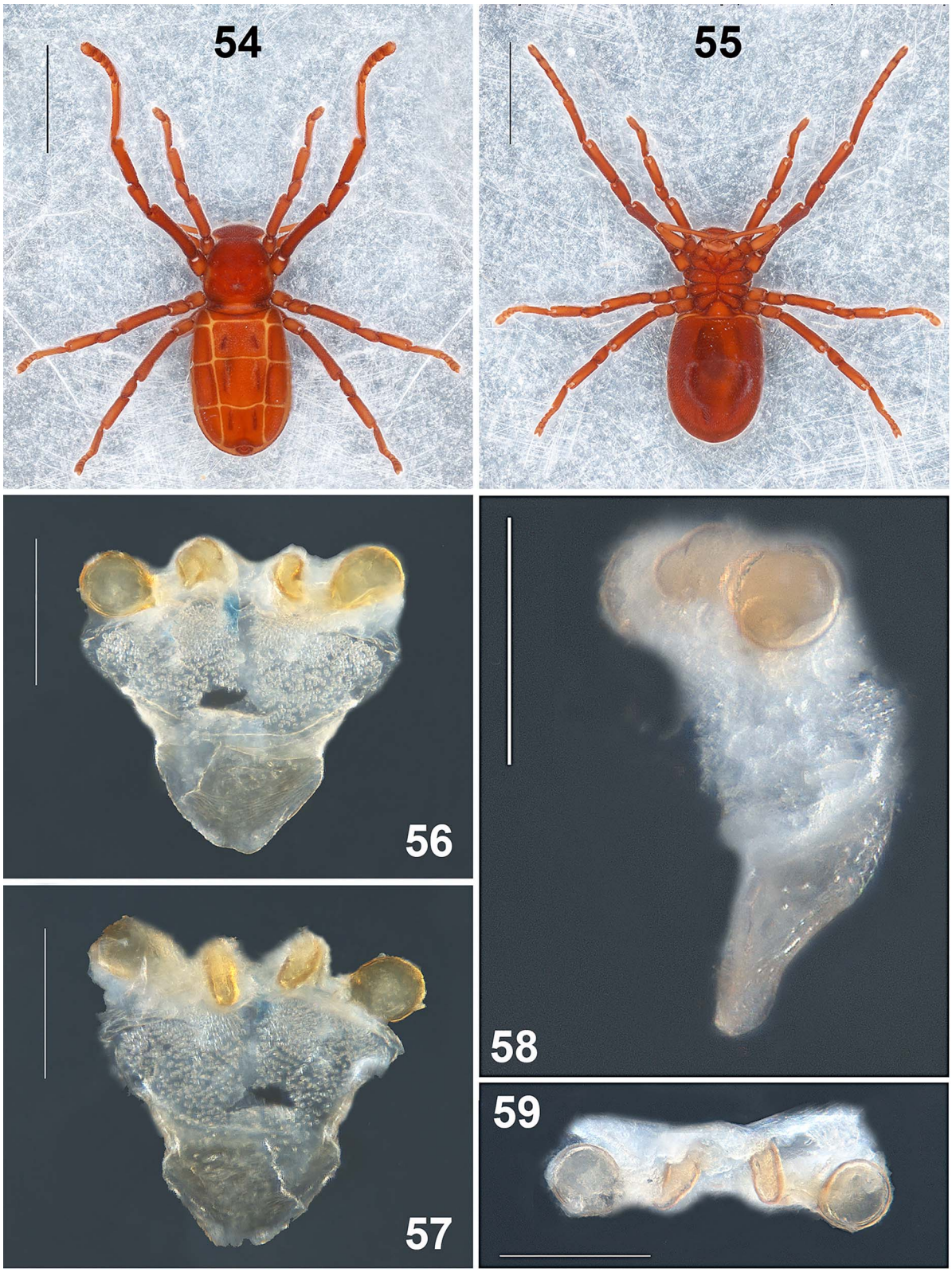

Figures 54–59.—*Pseudocellus pelaezi*, female 2. 54–55. Habitus, dorsal and ventral views. 55–58. Spermathecae, anterior, posterior, lateral and dorsal views, respectively. Scale bars: 54–55 = 2 mm; 56–59 = 0.2 mm.

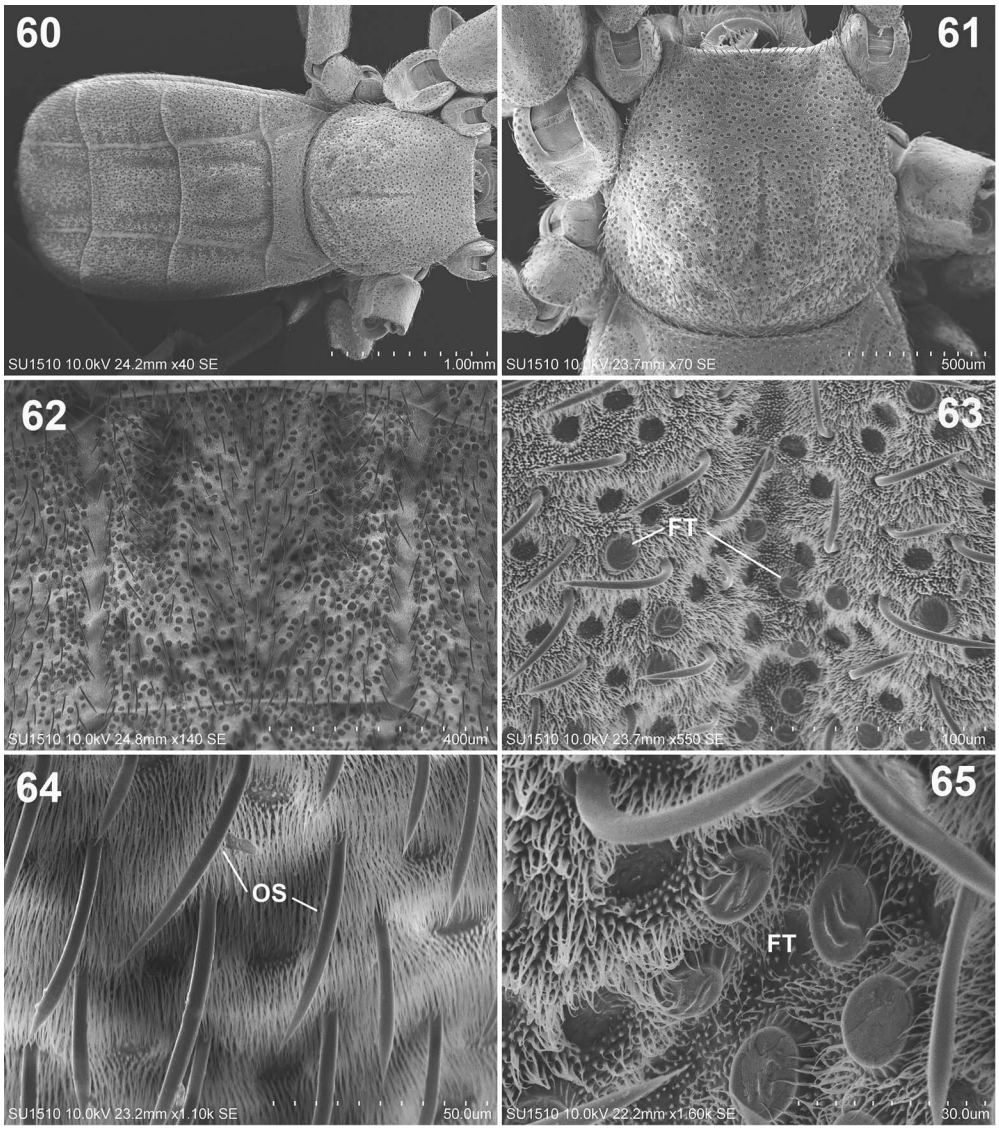

Figures 60–65.—*Pseudocellus pelaezi*, male morpho 1 (M1). 60. Habitus, dorsal view. 61. Carapace, dorsal view. 62. Detail of tergite XII of opisthosoma. 63. Carapace, cuticular detail, showing the flattened tubercles (FT) on the median groove. 64. Detail of the ordinary setae (OS) on dorsal carapace surface. 65. Detail of FT on median groove of the carapace.

Examined material.—MEXICO*:* Tamaulipas 3 ♂♂, 3 ♀♀, 1 deutonymph, 1 tritonymph, (CARCIB-Ri001) [17.x.2019; A. Valdez, B. Huber A. Cabrera Cols.] from Outside of Cueva Ojo de Agua, Ejido Ojo de Agua, Municipality Gómez Farias, Biosphere Reserve El Cielo (23.0376°, -99.1293°, 121 m), tropical rainforest (day collecting). 13♂♂, 16♀♀, 1 larva, 1 protonymph, 15 deutonymphs, and 20 tritonymphs (CNAN) [23.iv.2016; G. Montiel, J. Cruz, R. Monjaraz, G. Contreras, D. Guerrero, K. Arreguin Cols.] from same locality (day collecting). 3♀♀, and 4 deutonymphs (CNAN) [08.ix.2019; D. Guerrero, G. Montiel, G. Contreras, R. Monjaraz Cols.] from same locality (day collecting).

Diagnosis and description.—See Coronado-Gutiérrez (1970) and Pittard & Mitchell (1972) for complete diagnosis and description.

Natural History.—The specimens collected for this study (Figs. 93–98) were collected in a tropical rain forest at 121 m above sea level (Fig. 99). The specimens were found outside of a karstic cave, Cueva Ojo de Agua, Municipality Gómez Farias, which belongs to the Biosphere Reserve El Cielo, Tamaulipas. The specimens were collected on the ground, mainly under rocks but also in the leaf litter (Figs. 99-101, red arrows).

Distribution.—Biosphere Reserve Sierra del Abra Tanchipa, San Luis Potosi and Tamaulipas, and Biosphere Reserve El Cielo, Tamaulipas, Mexico (Fig. 102). Reddell (1981) mentions that *C. pelaezi* is known from both cave and epigean sites in the Sierra de El Abra, San Luis Potosi and Tamaulipas, and from epigean sites in the Sierra de Guatemala, Tamaulipas.

DISCUSSION

The evolutionary aspects of within male's dimorphism and polymorphism has been widely studied in several animal groups. Specifically in arthropods, this topic has been researched in

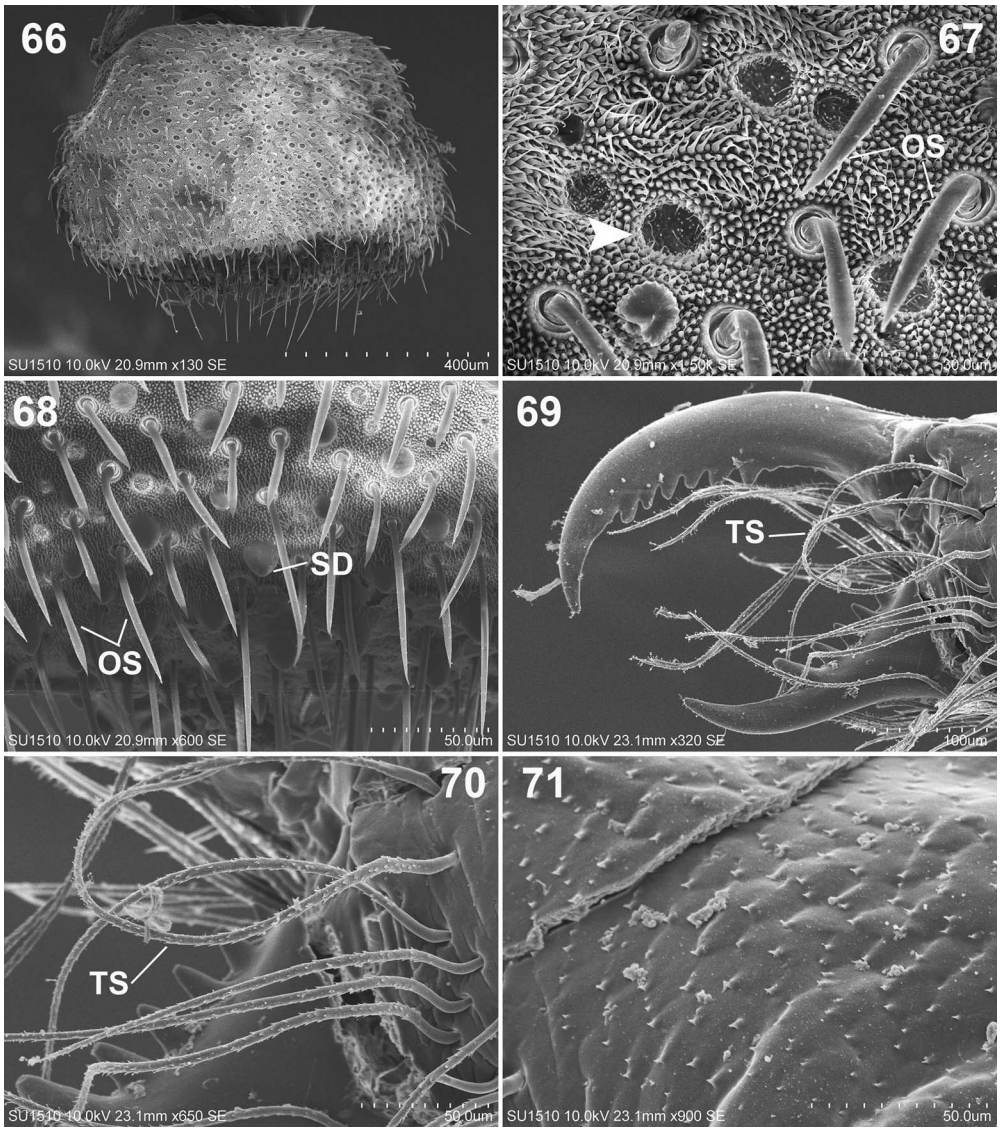

Figures 66–71.—*Pseudocellus pelaezi*, male morpho 1 (M1). 66. Cucullus, dorsal view. 67. Detail of pits on the cucullus (arrow), showing the ordinary setae (OS). 68. Detail of the OS and the dome-like tubercles (SD) on apical region of the cucullus. 69. Right chelicera, dorsal view, showing the tree-like setae (TS). 70. Detail of the TS on chelicera. 71. Detail of the chelicera surface.

insects, crustaceans, and even arachnids such as spiders, mites, pseudoscorpions, harvestmen, and short-tailed whipscorpions (de Armas 1989; Radwan & Bogacz 2000; Vanacker et al. 2003; Buzatto et al. 2011; Zatz et al. 2011; Santos et al. 2013; Zeh & Zeh 2013; Monjaráz-Ruedas & Francke 2015). In arachnids such as harvestman, trimorphisms have been described and evidence provided that complex polymorphisms in sexually-selected traits such as the male chelicerae exist in at least in two genera of the family Neopilionidae (Powell et al. 2020). In the smaller arachnid orders such as short-tailed whipscorpions (Schizomida), some species exhibit dimorphism among adult males. Some male palps are very similar to the palps of juvenile and female specimens, and these males are known as *homeomorphic* males (de Armas 1989; Santos et al. 2013; Monjaráz-Ruedas & Francke 2015). In contrast, *heteromorphic* males show palps widely elongated, approximately 2–3 times longer than those of adult females and homeomorphic males (de Armas 1989).

Similar to these whipscorpions, *P. pelaezi* studied herein can be considered a dimorphic species based on the differential morphology of the males, with homeomorphic (morpho 1-M1) and heteromorphic males (morpho 2-M2). In this case, the intrasexual differences are found in the femora II of the males, an important secondary sexual feature. Some males have homeomorphic femora II (thin femora), while others have heteromorphic femora II (wide femora). Even Pittard & Mitchell (1972) mentioned: "the femur II is often markedly sexually dimorphic, the male usually identifiable by its enlarged femur. In most specimens, this joint is at least twice as large in diameter as that of the female. However, in some specimens the femur is about the same thickness as the female's so that upon superficial examination these individuals appear to be females." For *P. pelaezi*, the primary sexual features such as the male copulatory apparatus of the leg III and the spermathecae shape of the females are still robust characters for species delimitation,

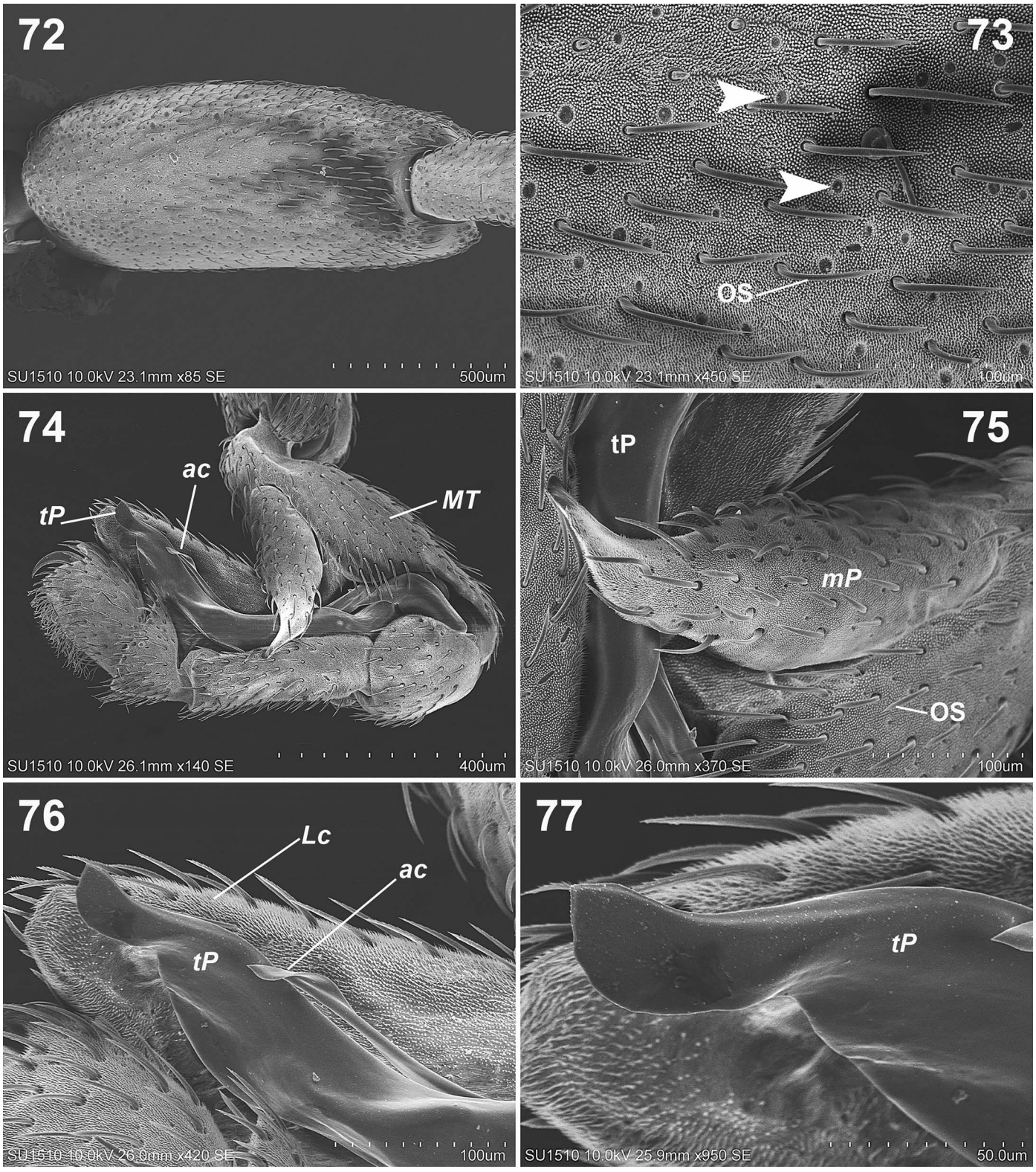

Figures 72–77.—*Pseudocellus pelaezi*, male morpho 2 (M2). 72. Femur II, dorsal view. 73. Cuticular detail of femur II showing the pits (arrows) and the ordinary setae (OS). 74. Right leg III (copulatory apparatus), prolateral view. 75. Detail of the metatarsal process (mP). 76. Detail of the tarsal process (tP) and accessory piece (ac) of the copulatory apparatus. 77. Apical detail of the tP of the copulatory apparatus.

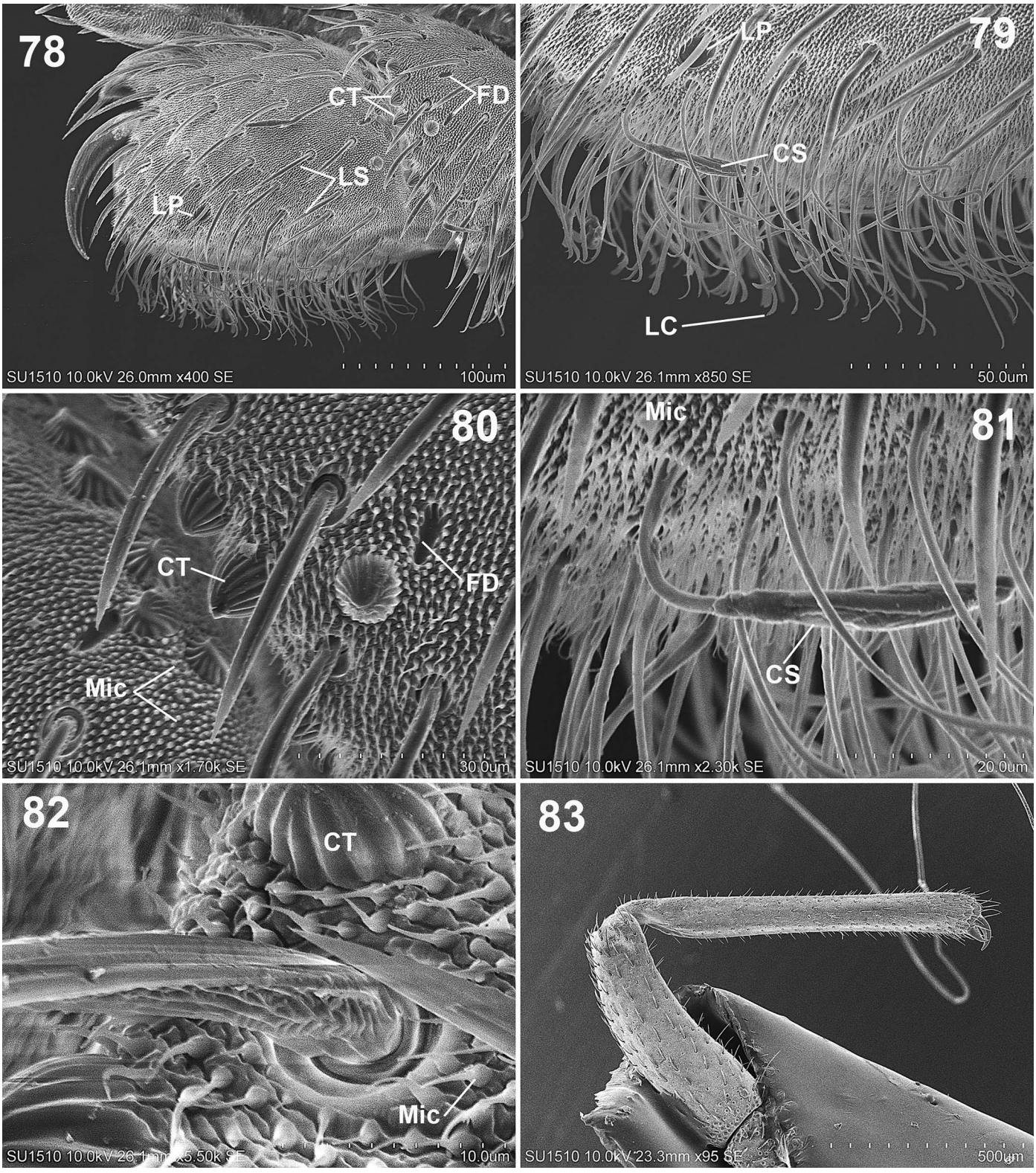

Figures 78–83.—*Pseudocellus pelaezi*, male morpho 2 (M2). 78. Tarsal claws of leg III showing the lamellar setae (LS). 79. Detail of the long curved-tip setae (LC), long and porous setae (LP), and curved and wide setae (CS) on ventral part of tarsus IV of leg III. 80. Detail of the conical tubercles (CT) and flat depressions (FD) on distal part of tarsus III of leg III. 81. Detail of the CS on ventral part of tarsus IV of leg III. 82. Detail of the CT and the microtrichia (Mic) on of tarsus III of leg III. 83. Right pedipalp, retrolateral view.

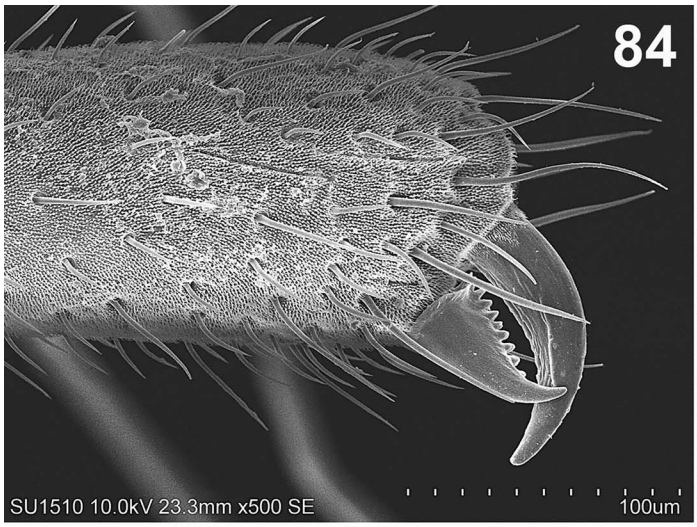

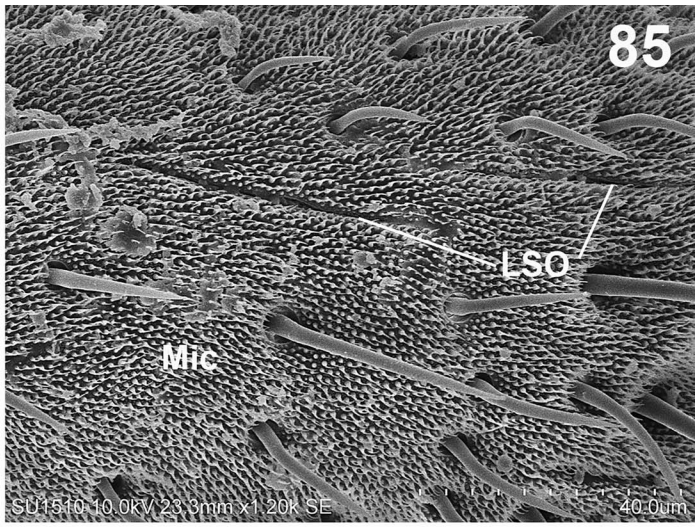

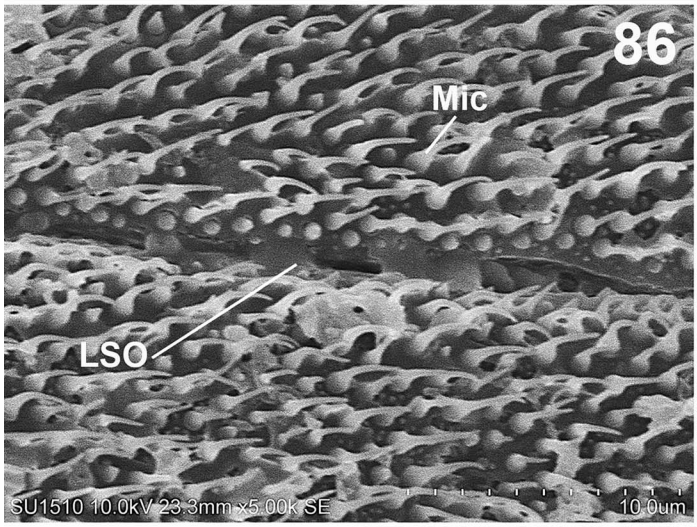

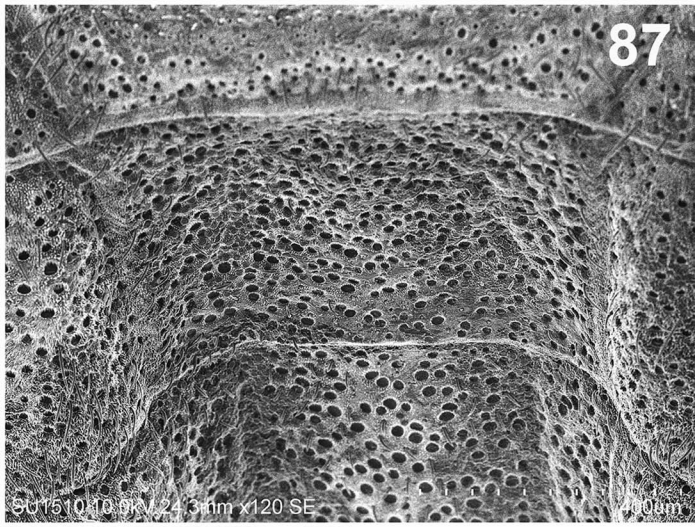

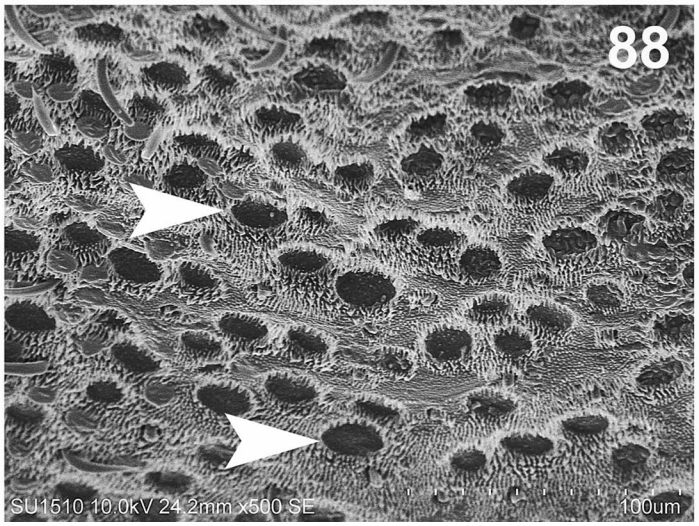

Figures 84–88.—*Pseudocellus pelaezi*, male morpho 2 (M2) (84–86). 84. Detail of the movable and fixed claws of right pedipalp, retrolateral view. 85. Detail of the cuticular surface of right pedipalp showing the mechanoreceptor long slit organs (LSO). 86. Detail of the LSO and microtrichia (Mic). Female: 87. Tergite XII of opisthosoma. 88. Detail of the pits (arrows) of tergite XII.

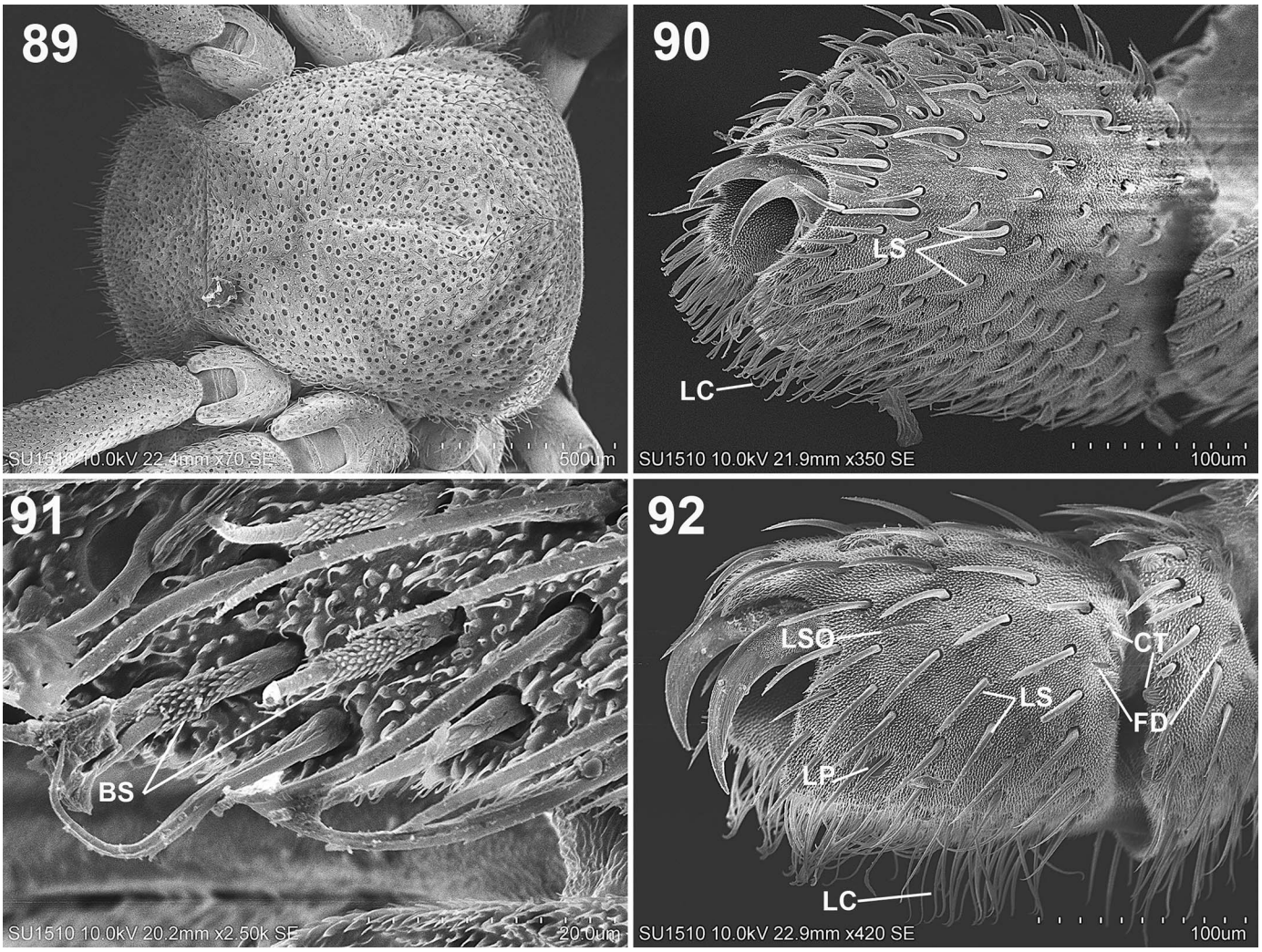

Figures 89–92.—*Pseudocellus pelaezi*, female. 89. Carapace, dorsal view. 90. Tarsus I of leg I showing the lamellar setae (LS) and the claws. 91. Detail of the barbed setae (BS) on ventral part of tarsus V of leg II. 92. Tarsus IV of leg III showing the claws. Abbreviations: LSO: mechanoreceptor long slit organs. LP: long and porous setae. CT: conical tubercles. FD: flat depressions. LC: long curved-tip setae.

despite the presence of dimorphic males in the shape of the femora II, a secondary sexual character, as well as some somatic differences such as carapace and cucullus shape.

Over the last few decades, the use of DNA barcoding markers has been a powerful and useful tool to understand the diversity in diverse groups and to recognize underestimated and cryptic diversity. This technique is widely used to assign individual organisms into pre-existing species and to designate new species based on species delimitation. For a long time and even nowadays, taxonomists have used only traditional morphology and/or somatic characters for species identification and delimitation (Rannala & Yang 2020). However, plastic characters, i.e., characters with high morphological variation such as intrasexual variation in males, a paucity of distinctive morphological traits among species, and morphological stasis due to environmental selection are present in some groups of organisms, making species delimitation based on morphological characters alone very difficult (Bickford et al. 2007; Carstens et al. 2013). The use of CO1 for DNA barcoding can be helpful for species diagnosis given that sequence divergences are normally much lower among individuals of the same species than between closely related species (Hebert et al. 2004). However, species delimitation based only on molecular data (in this case CO1) can rarely be achieved, and additional types of evidence are needed to recognize genetic lineages as distinct species (Hamilton et al. 2011). In the case of *P. pelaezi*, the genetic variation at the CO1 locus does not support the existence of two groups or putative species/lineages. Although two shallow genetic groups were recovered from the same population (Fig. 1, group 1 and 2), these groupings do not correspond with the two morphotypes found (M1 and M2), with both morphos being found within both genetic groupings (Fig. 1). Furthermore, no somatic differences were observed among females across the two genetic groupings, as the spermathecae had the same morphology in all the specimens analyzed.

We hypothesized that the genetic differences among the specimens belonging to the same population of *P. pelaezi* might correspond to a genetic variation or maybe genetic polymorphism as has been previously reported in other arthropods. In the small marine isopod (*Paracerceis sculpa*) that inhabits intertidal sponges, females mate with large fighter

Figures 93–98.—Live specimens of *Pseudocellus pelaezi* from Outside of Cueva Ojo de Agua, Ejido Ojo de Agua, Municipality Gómez Farias, Biosphere Reserve El Cielo, Tamaulipas, Mexico. 93. Adults and immatures specimens in aggregation. 94. Adult female. 95–96. Tritonymph and deutonymph respectively. 97–98. Larva and tritonymph respectively. Photos by G. Montiel-Parra (93–96), and J. Quirino Arreguín (97–98).

males, intermediate-sized males mimic females, and even smaller males act as sneaker males. Shuster & Wade (1991) conclude that the three phenotypes are a result of three alleles at a single autosomal locus. In the swordtail (*Xiphiphorus nigrensis*), three alleles at a single Y-locus are thought to determine small, intermediate, and large males that sneak, sneak and court, and court females, respectively (Ryan et al. 1992).

The morphological dimorphism found within the same population of *P. pelaezi* might be a direct effect of sexual competition among males to mate with females; however more studies are needed to understand its causes. Males across a variety of biological groups have highly exaggerated sexual structures used to enhance their mating success with the females. These exaggerated structures include ornaments that are used to signal male quality to potential female mates and structures to rival conspecific males (Parker 1974; Hurd 2006). This has been previously observed even with arachnids; opilionids present several examples showing how intra-sexual polymorphism in male structures such as the chelicerae help in contests among males (Buzatto et al. 2011; Powell et al. 2020).

As far we know, there is no evidence of male-male fights in ricinuleids; the role of the male femora II in mating is unknown. The second pair of legs in ricinuleids is commonly used as a sensory device mostly while the animal walks, confirming the structure's importance for orientation in ricinuleids (Platnick & Pass 1982). In their morphological study of *P. pelaezi*, Pittard & Mitchell (1972) confirmed that the first two pairs of legs, as well as the palps and the chelicerae, are equipped with numerous chemo-, mechano-, thermo- and hygroreceptors that act as the main sensing devices in ricinuleids. García et al. (2015) present a detailed work about the behavioral repertoire and its variation across day and night within the Neotropical ricinulei *Cryptocellus narino* Platnick & Paz, 1979 under laboratory conditions. They describe fight interactions only for food, but

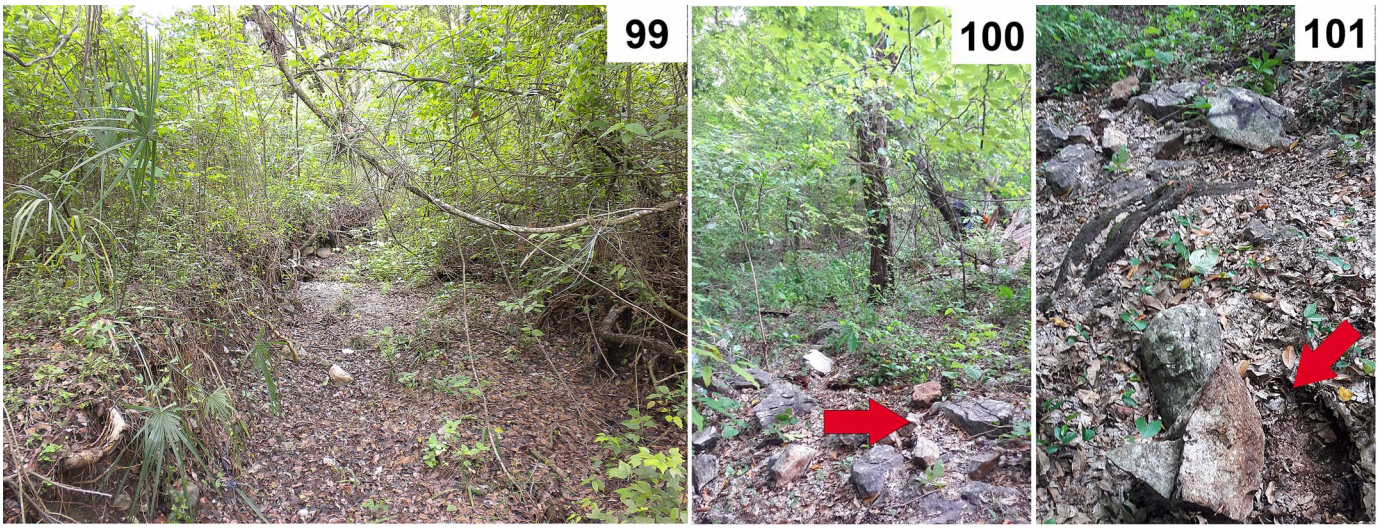

Figures 99–101.—Habitat and microhabitat of *Pseudocellus pelaezi*. 99. Tropical rain forest, Outside of Cueva Ojo de Agua, Ejido Ojo de Agua, Municipality Gómez Farias, Biosphere Reserve El Cielo, Tamaulipas, Mexico. 100–101. Medium boulders on the ground where the specimens were collected (red arrows indicate the specific microhabitat). Photos by G. Montiel-Parra (99), and A. Valdez-Mondragón (100–101).

do not describe fight interactions among males for mating with females. Drastic variation among males in weapon shape and size, leading to complex polymorphism of such as structures is a relatively new discovery (Powell et al. 2020).

In conclusion, although morphological and molecular evidence was provided for the very first time in Ricinulei to explain the male dimorphism, the main aspect needed to understand the dimorphism in *P. pelaezi* is to study and evaluate the sexual behavior in relation to the genetic evidence, including more specimens from several populations. This will illuminate whether such dimorphism and/or genetic variation is correlated with sexual competition, or alternatively maybe we are underestimating the diversity of sympatric species as has been previously reported by Reddell (1981) and Valdez-Mondragón et al. (2018).

ACKNOWLEDGMENTS

The first author thanks the program "Investigadores por México, ex Cátedras CONACyT", Consejo Nacional de Humanidades, Ciencia y Tecnología (CONAHCyT), Mexico for scientific support for project No. 59: "Laboratorio Regional de Biodiversidad y Cultivo de Tejidos Vegetales (LBCTV) del Instituto de Biología (IBUNAM), Tlaxcala." The first author also thanks SEP-CONAHCyT for financial support of the project of Basic Science (Ciencia Básica) 2016, No. 282834. We thank the students of the Laboratory of Arachnology (LATLAX) and the National Collection of Arachnids (CNAN), IBUNAM, Mexico for their help in the collection of specimens in the field. We are grateful to Ing. Jean-Louis Lacaille Muzquiz, Lic. Javier Olivos

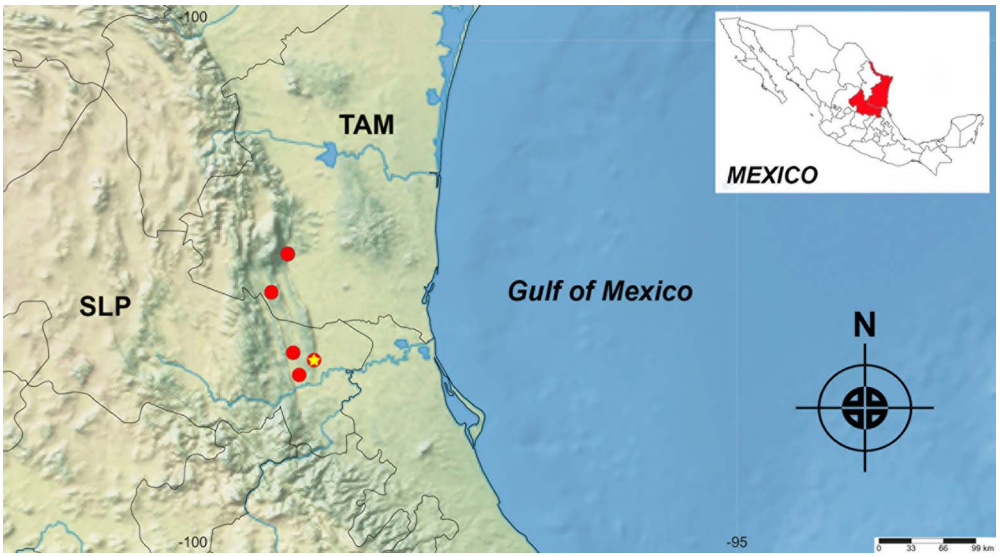

Figure 102.—Known records of *Pseudocellus pelaezi* from northeastern Mexico. Type locality: Cueva del Taninul, San Luis Potosi (yellow star). Abbreviations: SLP = San Luis Potosi, TAM = Tamaulipas.

Martínez, and Biól. Mario Álvarez of the Centro Interpretativo Ecológico for their help during fieldwork in 2016. We are grateful to CIBNOR S. C. for the facilities provided to complete this research. We thank Dr. Jesús A. Cruz López and M.Sc. Berenit Mendoza Gárfias for the SEM photomicrographs and MSc. Laura Márquez Valdelamar for the molecular sequencing of the samples. We thank Brett O. Butler for the English language review of the manuscript, and the reviewers for their comments and suggestions that improved the manuscript. The specimens were collected under Scientific Collector Permit FAUT-0309 and FAUT-0027 from the Secretaría de Medio Ambiente y Recursos Naturales (SEMARNAT).

LITERATURE CITED

Andersson M. 1994. Sexual Selection. Princeton University Press, Princeton, NJ.

Barraclough TG, Harvey PH, Nee S. 1995. Sexual selection and taxonomic diversity in passerine birds. *Proceedings of the Royal Society of London, Series B* 259:211–215.

Bickford D, Lohman DJ, Sodhi NS, Ng PKL, Meier R, Winker L. et al. 2007. Cryptic species as a window on diversity and conservation. *Trends in Ecology & Evolution* 22:148–155.

Botero-Trujillo R, Sain CE, Prendini L. 2021a. Systematics of the "giant" ricinulei (Ricinoididae: Ricinoides) of West Africa, with descriptions of five new species and comparative morphology of the male copulatory apparatus. *Bulletin of the American Museum of Natural History* 448(5):1–68.

Botero-Trujillo R, Carvalho L, Florez E, Prendini L. 2021b. Four new species of "hooded tickspiders" (Ricinulei, Ricinoididae) from South and Central America, with clarification of the identity of *Cryptocellus leleupi* Cooreman, 1976. *American Museum Novitates* 3976:1–35.

Buzatto BA, Requena GS, Lourenco RS, Munguía-Steyer R, Machado G. 2011. Conditional male dimorphism and alternative reproductive tactics in a Neotropical arachnid (Opiliones). *Evolutionary Ecology* 25:331–349.

Carstens BC, Pelletier TA, Reid NM, Satler J. 2013. How to fail at species delimitation. *Molecular Ecology* 22:4369–4383.

Coronado-Gutiérrez L. 1970. Estudio de un *Cryptocellus* de cavernas de México (Arachnida: Ricinulei). *Ciencia, México* 27:47–62.

Darwin C. 1871. The Descent of Man; and Selection in Relation to Sex. Second Edition, Crowell, New York, NY.

de Armas LF. 1989. Adiciones al orden Schizomida (Arachnida) en Cuba. *Poeyana* 387:1–45.

de Armas LF. 2017. Cuatro especies nuevas de *Pseudocellus* de Cuba (Arachnida: Ricinulei). *Revista Ibérica de Aracnología* 30:87–99.

Folmer O, Black M, Hoeh W, Lutz R, Vrijenhoek RC. (135 co-authors). 1994. DNA primers for amplification of mitochondrial cytochrome c oxidase subunit I from diverse metazoan invertebrates. *Molecular Marine Biology and Biotechnology* 3:294–299.

García LF, Torrado-León E, Talarico G, Peretti AV. 2015. First characterization of the behavioral repertory in a ricinuleid: *Cryptocellus narino* Platnick & Paz 1979 (Arachnida, Ricinulei, Ricinoididae). *Journal of Insect Behavior* 28:447–459.

Gertsch WJ. 1971. Three new ricinuleids from Mexican caves (Arachnida, Ricinulei). *Bulletin of the Association for Mexican Cave Studies* 4:127–135.

Gross MR. 1996. Alternative reproductive strategies and tactics: diversity within sexes. *Trends in Ecology & Evolution* 11:92–98.

Hall TA. 1999. BioEdit: a user-friendly biological sequence alignment editor and analysis program for Windows 95/98/NT. In Nucleic acids symposium series (Vol. 41, No. 41, pp. 95–98).

Hamilton CA, Formanowicz DR, Bond JE. 2011. Species delimitation and phylogeography of *Aphonopelma hentzi* (Araneae, Mygalomorphae, Theraphosidae): cryptic diversity in North American tarantulas. *PloS One* 6(10):e26207.

Harvey MS. 2003. Catalogue of the Smaller Arachnid Orders of the World. CSIRO Publishing, Collinwood, Victoria, Australia.

Hebert PDN, Penton EH, Burns JM, Janzen DH, Hallwachs W. 2004. Ten species in one: DNA barcoding reveals cryptic species in the Neotropical skipper butterfly *Astraptes fulgerator*. *Proceedings of the National Academy of Sciences of the United States of America* 101:14812–14817.

Huber BA. 2021. Beyond size: sexual dimorphisms in pholcid spiders. *Arachnology* 18:656–677.

Hurd PL. 2006. Resource holding potential, subjective resource value, and game theoretical models of aggressiveness signalling. *Journal of Theoretical Biology* 241:639–648.

Katoh K, Toh H. 2008. Recent developments in the MAFFT multiple sequence alignment program. *Briefings in Bioinformatics* 9:286–298.

Kumar S, Stecher G, Li M, Knyaz C, Tamura K. 2018. MEGA X: molecular evolutionary genetics analysis across computing platforms. *Molecular Biology and Evolution* 35:1547.

Monjaraz-Ruedas R, Francke OF. 2015. Taxonomic revision of the genus *Mayazomus* Reddell & Cokendolpher, 1995 (Schizomida: Hubbardiidae), with description of five new species from Chiapas, Mexico. *Zootaxa* 3915:451–490.

Nolasco S, Valdez-Mondragón A. 2022. To be or not to be: Integrative taxonomy and species delimitation in the daddy long-legs spiders of the genus *Physocyclus* (Araneae, Pholcidae) using DNA barcoding and morphology. *ZooKeys* 1135:93.

Parker GA. 1974. Assessment strategy and the evolution of animal conflicts. *Journal of Theoretical Biology* 47:223–243.

Pittard K, Mitchell RW. 1972. Comparative morphology of the life stages of *Cryptocellus pelaezi* (Arachnida, Ricinulei). Texas Tech University. Texas Tech Press, Lubbock, Texas 1:1–77.

Platnick NI, Pass G. 1982. On a new Guatemalan *Pseudocellus* (Arachnida, Ricinulei). *American Museum Novitates* 2733:1–6.

Powell EC, Painting CJ, Hickey AJ, Holwell GI. 2020. Defining an intrasexual male weapon polymorphism in a New Zealand harvestman (Opiliones: Neopilionidae) using traditional and geometric morphometrics. *Biological Journal of the Linnean Society* 130:395–409.

Radwan J, Bogacz I. 2000. Comparison of life-history traits of the two male morphs of the bulb mite, *Rhizoglyphus robini*. *Experimental and Applied Acarology* 24:115–121.

Rannala B, Yang Z. 2020. Species Delimitation. Phylogenetics in the Genomic Era, No commercial publisher, Authors open access book, 5.5:1–5.5:18.

Reddell JR. 1981. A Review of the Cavernicole Fauna of Mexico, Guatemala, and Belize.

Rozen S, Skaletsky H. 1999. Primer3 on the WWW for general users and for biologist programmers. *Bioinformatics Methods and Protocols* 1:365–386.

Ryan MJ, Pease CM, Morris MR. 1992. A genetic polymorphism in the swordtail *Xiphiphorus nigrensis*: testing the prediction of equal fitnesses. *American Naturalist* 139:21–31.

Salvatierra L, Tourinho AL. 2016. The integumentary ultrastructure of *Cryptocellus bordoni* Dumitresco and Jurvara-Bals, 1976 (Arachnida, Ricinulei). *Micron* 81:48–66.

Santos AJ, Ferreira RL, Buzatto BA. 2013. Two new cave-dwelling species of the short-tailed whipscorpion genus *Rowlandius* (Arachnida: Schizomida: Hubbardiidae) from Northeastern Brazil, with comments on male dimorphism. *PLoS One* 8(5):e63616.

Selden PA. 1992. Revision of the fossil ricinuleids. *Transactions of the Royal Society of Edinburgh: Earth Sciences* 83:595–634.

Shorthouse DP. 2010. SimpleMappr, an online tool to produce publication-quality point maps. Online at http://www.simplemappr.net

Shuster SM, Wade MJ. 1991. Equal mating success among male reproductive strategies in a marine isopod. *Nature* 350:608–610.

Talarico G, Palacios-Vargas JG, Fuentes-Silva M, Alberti G. 2006. Ultrastructure of tarsal sensilla and other integument structures of two *Pseudocellus* species (Ricinulei, Arachnida). *Journal of Morphology* 267:441–463.

Teruel R, de Armas LF. 2008. Nuevo *Pseudocellus* Platnick 1980 de Cuba oriental y nuevos registros de *Pseudocellus paradoxus* (Cooke 1972) (Ricinulei: Ricinoididae). *Boletín de la Sociedad Entomológica Aragonesa* 43:29–33.

Tuxen SL. 1974. The African genus *Ricinoides* (Arachnida, Ricinulei). *Journal of Arachnology* 1:85–106.

Valdez-Mondragón A, Cortez-Roldán MR. 2021. COI mtDNA barcoding and morphology for the description of a new species of ricinuleid of the genus *Pseudocellus* (Arachnida: Ricinulei: Ricinoididae) from El Triunfo Biosphere Reserve, Chiapas, Mexico. *European Journal of Taxonomy* 778:1–25.

Valdez-Mondragón A, Francke OF. 2011. Four new species of the genus *Pseudocellus* (Arachnida: Ricinulei: Ricinoididae) from Mexico. *Journal of Arachnology* 39:365–377.

Valdez-Mondragón A, Francke OF. 2013. Two new species of ricinuleids of the genus *Pseudocellus* (Arachnida: Ricinulei: Ricinoididae) from southern Mexico. *Zootaxa* 3635:545–556.

Valdez-Mondragón A, Juárez-Sánchez AR. 2021. A new epigean species of ricinuleid of the genus *Pseudocellus* (Arachnida: Ricinulei: Ricinoididae) from a tropical sub-deciduous forest in Oaxaca, Mexico. *Journal of Arachnology* 48:329–338.

Valdez-Mondragón A, Cortez-Roldán MR, Campuzano-Granados EF. 2020. On the Mexican ricinuleids: a new species of the genus *Pseudocellus* (Arachnida: Ricinulei: Ricinoididae) from the cloud forest of Chiapas, Mexico. *Revista Mexicana de Biodiversidad* 91:1–12.

Valdez-Mondragón A, Francke OF, Botero-Trujillo R. 2018. New morphological data for the order Ricinulei with the description of two new species of *Pseudocellus* (Arachnida: Ricinulei: Ricinoididae) from Mexico. *Journal of Arachnology* 46:114–132.

Vanacker D, Maes L, Pardo S, Hendrickx F, Maelfait JP. 2003. Is the hairy groove in the gibbosus male morph of *Oedothorax gibbosus* (Blackwall 1841) a nuptial feeding device? *Journal of Arachnology* 31:309–315.

Wallace AR. 1889. Darwinism: An Exposition of the Theory of Natural Selection with Some of its Applications. Second Edition, MacMillan, London, UK.

Zatz C, Werneck RM, Macias-Ordonez R, Machado G. 2011. Alternative mating tactics in dimorphic males of the harvestman *Longiperna concolor* (Arachnida: Opiliones). *Behavioral Ecology and Sociobiology* 65:995–1005.

Zeh JA, Zeh DW. 2013. On the threshold of dispersal: hitchhiking on a giant fly favour exaggerated male traits in a male-dimorphic pseudoscorpion. *Biological Journal of the Linnean Society* 108:509–520.

Manuscript received 11 September 2023, revised 27 November 2023, accepted 10 January 2024.